SEDIMENTOLOGY the journal of the International Association of Sedimentologists

Sedimentology (2023) **70**, 1472–1495 doi: 10.1111/sed.13093

Factors controlling the morphology and internal sediment architecture of moats and their associated contourite drifts

HENRIETTE WILCKENS*,†, TILMANN SCHWENK*, THOMAS LÜDMANN‡, CHRISTIAN BETZLER‡, WENYAN ZHANG§, JIAYUE CHEN§, F. JAVIER HERNÁNDEZ-MOLINA¶, ALICE LEFEBVRE†, ANTONIO CATTANEO**, VOLKHARD SPIEß* and ELDA MIRAMONTES*,†

**Faculty of Geosciences, University of Bremen, 28359, Bremen, Germany (E-mail: cwilcken@uni-bremen.de)*

†MARUM – Center for Marine Environmental Sciences, University of Bremen, 28359, Bremen, Germany

‡Institute for Geology, University of Hamburg, 20146, Hamburg, Germany

§Institute of Coastal Systems, Helmholtz-Zentrum Hereon, 21502, Geesthacht, Germany

¶Department of Earth Sciences, Royal Holloway University of London, Egham, TW20 0EY, Surrey, UK

***UMR 6538 GEO-OCEAN, Ifremer, Univ Brest, CNRS, Univ, Bretagne-Sud, 29280, Plouzané, France*

Associate Editor – Jeff Peakall

ABSTRACT

The interaction of sedimentary systems with oceanographic processes in deep-water environments is not well understood yet, despite its importance for palaeoenvironmental reconstructions, and for a full understanding of source-to-sink sediment transport. The aim of this study is to improve the understanding of how contourite moats, elongated depressions formed by bottom currents associated with contourite drifts, develop and of the link between moat-drift system morphology and bottom current dynamics. This study provides a systematic comparison of 185 cross-sections of moat-drift systems distributed at 39 different locations worldwide, and a detailed analysis of the morphology of six moats that cover a wide range of typical geological and hydrodynamic settings. Additionally, *in situ* measured current data were analysed to better link hydrodynamics to moat morphology. The median of all profiles across all moat-drift systems reveals a 50 m relief, a width of 2.3 km, a relief to width ratio of 0.022, a slope angle of 6°, a drift angle of 3° and a concave-up shaped morphology. Moats can be over 100 km long. Some moats are driven by sediment erosion while others are depositional and primarily exist due to differential sedimentation inside the moat compared to the drift alongside the moat. A new sub-classification of moat-drift systems based on their stratigraphy is proposed. This classification distinguishes moats depending on the degree of erosion versus deposition. No relation is found between latitude and moat-drift morphology or stratigraphy in the analysed examples. The combined data indicate that a steeper slope focuses the current more than a gentle slope, resulting in an increase of the relief–width ratio and drift angle. Thus, this study provides new insights into the interaction of ocean currents with sedimentary morphology, which thereby affects the evolution of a poorly understood deep-water sedimentary system.

Keywords Bottom current, contourite drift, geomorphology, moats, sediment transport, sedimentary processes.

INTRODUCTION

Contourite moats are elongated depressions formed by ocean bottom currents and can be found parallel to the continental slope or other topographic obstacles (Rebesco *et al.*, 2014; Miramontes *et al.*, 2021). They are channel-like features, but in contrast to contourite channels that show erosion on both flanks, moats are not purely erosive. Moats are associated with separated mounded drifts forming parallel to one of the moat's sides (Rebesco *et al.*, 2014; Miramontes *et al.*, 2021). Moats are common in a variety of geological settings like open continental slopes, around seamounts and carbonate mounds (Rebesco *et al.*, 2014; Vandorpe *et al.*, 2014; Hebbeln *et al.*, 2016; Miramontes *et al.*, 2021). Because there is no moat without an associated drift, the authors consider them as one system that is referred to as a moat-drift system. Understanding the morphology of a moat also depends on the associated drift and thus moats and drifts cannot be studied independently. It has been proposed that moats are pathways for the transport of sediments and anthropogenic particles (such as microplastic) due to vigorous bottom currents, while particle accumulation mainly occurs on their associated contourite drifts where bottom current speed is lower (Rebesco *et al.*, 2014; Yin *et al.*, 2019; Kane *et al.*, 2020; Wilckens *et al.*, 2021). Analysing how sediment is transported within moats is important for understanding the heterogeneity of sediment distribution on the seafloor and the final fate of sediments in source-to-sink systems.

Moats and cold-water coral mounds form due to bottom currents and are often found next to one another (Hebbeln *et al.*, 2016). A better understanding of current behaviour over moats could also increase our understanding of how these ecosystems might develop in the future. This study does not consider a link between moats and plastered drifts. They do occur in the same contourite depositional systems and thus there is a special link, but the current dynamics are different and thus there is no direct link in the formation process (Miramontes *et al.*, 2021). Furthermore, moats and their associated separated mounded drifts provide records of past ocean conditions. The onset of contourite depositional systems, analysed based on morphological and seismic data, has been used in many different settings to identify large changes in global ocean circulation patterns, as well as the formation inside different water masses, and to understand relative changes in current speed over several thousands to millions of years (Hernández-Molina *et al.*, 2014; Uenzelmann-Neben *et al.*, 2017; Paulat *et al.*, 2019; Yin *et al.*, 2021). For quantitative reconstructions of speed mainly grain-size analyses have been used (McCave *et al.*, 1995, 2017; Wu *et al.*, 2021), with calibrations for quantitative palaeoreconstructions for some areas (McCave *et al.*, 2017). Taking several sediment cores is time-consuming and expensive, in particular in the deep sea. Efforts to link contourite morphology to the currents that formed them have progressed significantly in recent years due to more current measurements and high resolution modelling (Zhang *et al.*, 2016; Miramontes *et al.*, 2021; Rebesco *et al.*, 2021; Wilckens *et al.*, 2021). A better integration of the morphology in addition to sediment cores for the reconstruction of current speed could be faster, cheaper, applicable on larger scales and easier for reconstructing conditions over several million years.

There are different types of contourites, from which the morphology can be used for ocean current speed reconstructions, but so far the link between their morphology and the characteristics of currents is not very clear (McCave & Tucholke, 1986; Rebesco *et al.*, 2014; Miramontes *et al.*, 2019, 2021). It is hypothesized that moats are located under the main core of the current (Yin *et al.*, 2019; Wilckens *et al.*, 2021). This study intends to advance the understanding of the sedimentary processes that control moat formation and evolution. For decoding the sedimentary record of ocean currents, it is crucial to have a good understanding of the morphology and stratigraphy of the moat and the adjacent separated mounded drift, as well as the current conditions. Although moats have been recognized all over the world, there has not yet been a detailed analysis and comparison of the similarities and differences between them.

The Coriolis force together with the water pressure gradient determines the flow direction of a geostrophic current. It has been proposed that moats can only form on a continental slope where the Coriolis force deflects the current against the slope (McCave & Tucholke, 1986; Faugères *et al.*, 1999). The Coriolis force influences global ocean circulation by forcing the currents towards the right in the Northern Hemisphere and towards the left in the Southern Hemisphere. This can result in the formation of a contourite drift on the right side (looking

downstream) of the moat in the Northern Hemisphere and on the left side in the Southern Hemisphere (Faugères *et al.*, 1999; Llave *et al.*, 2001; Rebesco *et al.*, 2014). Thus, the Coriolis force is one parameter that influences where moats can form. However, it is unknown whether the Coriolis force also significantly influences the morphology of the moat. The Rossby number (Ro) is used to determine how important the Coriolis force is in a system (Davarpanah Jazi *et al.*, 2020). The Rossby number is defined as $Ro = U/fL$, with mean velocity U, Coriolis frequency f and length scale L. The Coriolis frequency f is defined as $f = 2\omega \sin(\varphi)$, with angular velocity ω and latitude φ. While the influence of the Coriolis force on moats is still unknown, its influence on submarine channels that develop due to downslope flowing turbidity currents has been demonstrated (Cossu *et al.*, 2010; Wells & Cossu, 2013; Allen *et al.*, 2022). For submarine channels, field observations show a latitudinal dependence on sinuosity (Wells & Cossu, 2013; Allen *et al.*, 2022). Moats do not meander and thus sinuosity is not a relevant parameter, but it is possible that the latitudinal dependence is preserved in the aspect ratio.

Contourites not only form due to geostrophic currents, but also due to other oceanographic currents that flow near the seafloor (Rebesco *et al.*, 2014). Around seamounts and other topographic obstacles moats can form not only on the side where the current is pushed against the slope, but also on the side where the Coriolis force deflects the current away from the slope (Hernández-Molina *et al.*, 2006; Hebbeln *et al.*, 2016; Chen *et al.*, 2022). It is suggested that the side where the Coriolis force is pushing the current towards the seamount is faster and leads to more erosion compared to the other side (Hernández-Molina *et al.*, 2006; Chen *et al.*, 2022). It remains unclear whether this concept is true for all sizes of seamounts. The pre-existing morphology could also affect the development of moats, and moat morphology is not only influenced by ocean currents but also by downslope movement of sediment, for example mud deposits from mud volcanoes (Vandorpe *et al.*, 2014). Therefore, understanding the dynamic feedback between the seafloor morphology and the bottom currents is of crucial importance in the study of contourite-moat systems.

This study systematically investigates the morphology and stratigraphy of moats and associated separated mounded drifts distributed worldwide. Then the measurements from different morphological parameters of the moats are used to test these hypotheses: (i) moat-drift systems have no specific aspect ratio because they are influenced by multiple processes; (ii) moat morphology changes with latitude because the Rossby number and Coriolis force depend on it; (iii) moat morphology correlates with water depth because of the influence of sediment availability and limited accommodation space; and (iv) moat aspect ratio and the steepness of the drift depend on the steepness of the slope at which the moat forms because the slope influences the hydrodynamics. Where available, current measurements from vessel-mounted Acoustic Doppler Current Profilers (VM-ADCP) were also used to better understand the link between moat-drift system morphology and hydrodynamics.

MATERIALS AND METHODS

Measurements of moat parameters

Moats from different locations around the world (Fig. 1) were analysed to provide a synthesis of their occurrence in the literature and identify common characteristics and genetic features. The location of all moats included in this study, and the key references of the previous studies in these areas, can be found together with the origin of the data sets used in the analysis in the supplementary material (Table S1). For the comparison of different morphologies of moat-drift systems around the world, the following morphological parameters were measured: width, relief, slope angle, drift angle and, where possible, the length of moats (Fig. 2). The moat trough is the deepest point inside the moat and the drift crest the shallowest point of the contourite drift. The moat width is defined as the horizontal distance between the drift crest and the slope. The relief is defined as the vertical distance between moat trough and drift crest. The slope angle and the drift angle are the average gradient in both flanks of the moat: (i) between the moat trough and the slope; and (ii) between the moat trough and the drift crest (Fig. 2). In total, 45 different stratigraphic sections were analysed (using seismo-acoustic data) and 185 cross-sections (from bathymetric data) of moat-drift systems were measured. For 50 moats, one cross-section was measured and for 19 moats multiple cross-sections were measured, that account in total for 126 cross-

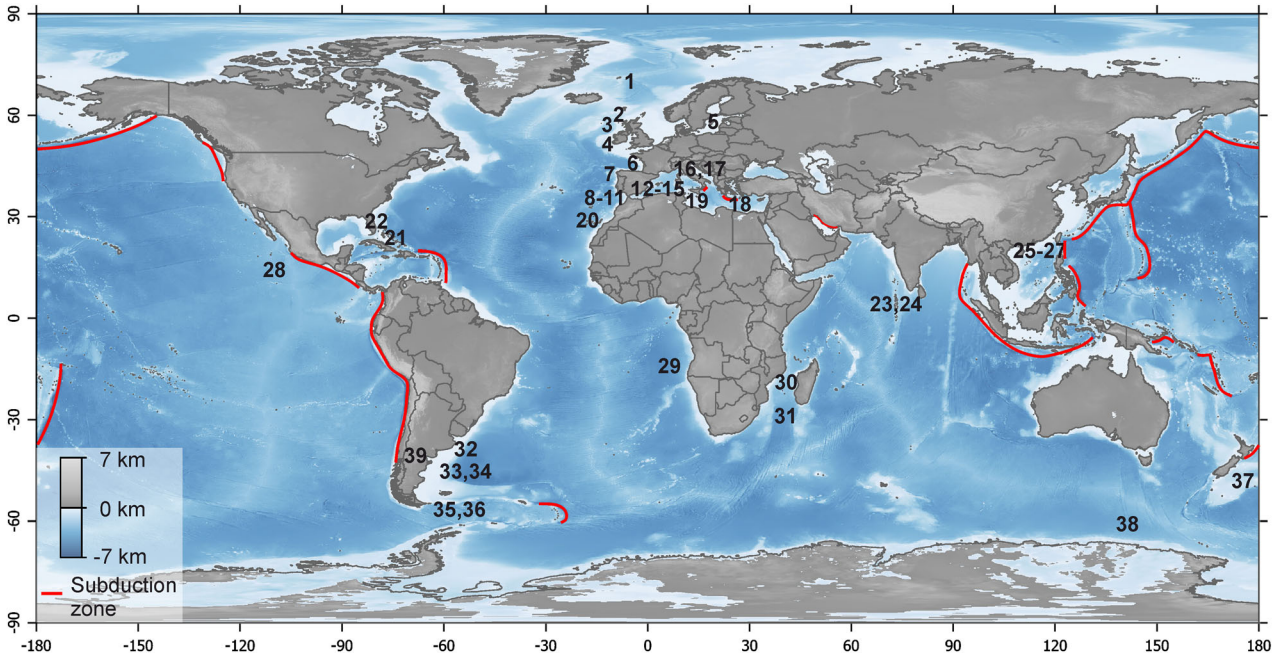

Fig. 1. Location of moats considered in this study: 1 – NW Barents Sea; 2 – North Rockall Trough; 3 – Rockall Trough (Seamount); 4 – Ireland; 5 – Baltic Sea; 6 – Gulf of Biscay; 7 – Galicia; 8–11 – Gulf of Cadiz; 12–13 – Adriatic Sea; 14 – Balearic Sea; 15 – Tyrrhenian Sea; 16–17 – Alboran Sea; 18 – Aegean Sea; 19 – Malta; 20 – Lanzarote; 21–22 – Bahamas; 23–24 – Maldives; 25–26 – South China Sea; 28 – Pacific Ocean (Clarion–Clipperton Zone); 29 – Angola (Anna Ridge); 30 – Mozambique; 31 – Madagascar; 32–34 – Argentina; 35–36 – Patagonia; 37– New Zealand; 38 – Antarctica; 39 – Lago Cardiel (Lake in Argentina). See Table S1 of the supplementary material for references. The subduction zones are adapted from van Keken *et al.* (2011).

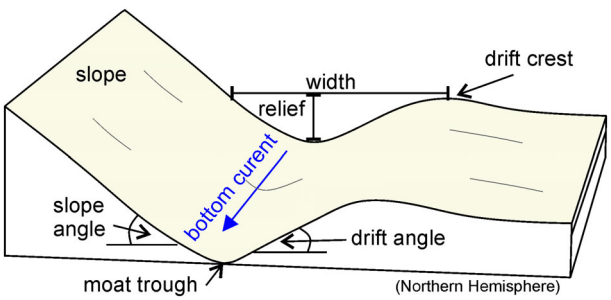

Fig. 2. Cross-section of a moat-drift system where the measured parameters (width, relief, slope angle and drift angle) are defined.

sections. For the statistics presented here, all datapoints were used, to also account for changes within one moat-drift system. To check if there is a bias in the statistics the median relief, width, ratio, slope angle and drift angle with all data points and with just one cross-section from each system were calculated. The relative deviation for all parameters is below 8%.

The sizes of previously published moats were measured from the seismic or sub-bottom profiler cross-sections that were published either in a journal or on the GeoMapApp (www.geomapapp.org) (Table S1 and PANGAEA database). In cases in which multibeam data are available, the parameters from the bathymetric map were measured. The consistency of the measurements was checked using both methods (from the bathymetry and from the seismic profiles) on the Ewing Terrace Moat 2 (ET Moat 2) offshore North Argentina and the same results were found. The authors are therefore confident that all of the measurements are comparable.

In the statistical analyses, the influence of one parameter on the morphological moat parameters (relief, width and aspect ratio) is tested. To understand which parameters are most relevant for shaping the moat-drift system, they are tested one at a time. However, this means that parameters that only have a small influence on the moat-drift system cannot be identified. One of the main interests is to determine how the strength of the Coriolis force influences the moat morphology, which is why multiple morphological parameters were measured and correlated with the latitude. The Coriolis frequency is higher at high latitudes and becomes zero at the

Table 1. Summary of the bathymetry data.

Area	Cruise	Reference	Grid cell size
North Argentina (SW Atlantic Ocean)	Cruise SO260 onboard the *R/V SONNE* in 2018	Kasten *et al.* (2019); Wilckens *et al.* (2021)	25 m
Mozambique Basin (SW Indian Ocean)	Cruise -MOZ2 onboard the *R/V L'Atalante* in 2014	Robin & Droz, 2014; Cécile & Laurence, 2014; Miramontes *et al.*, 2021	30 m
Corsica Trough (northern Tyrrhenian Sea, NW Mediterranean Sea)	Cruise PRISME2 onboard the *R/V L'Atalante* and cruise PRISME3 onboard the *R/V Pourquoi pas?* Survey in 2013	Cattaneo (2013a,b), Miramontes *et al.* (2016)	15 m
Offshore Galicia (NW Spain, NE Atlantic Ocean)	Cruise M84/4 onboard the *R/V Meteor* in 2011	Hanebuth *et al.* (2011), Hanebuth *et al.* (2015)	75 m
Offshore the Santaren Channel in the Bahamas	Cruise M95 onboard the *R/V Meteor* in 2013	Betzler *et al.* (2014a,b), Lüdmann *et al.* (2016)	200 m
Gulf of Cadiz	Cruise CADIPOR 1 + 2 onboard the *R/V Belgica* in 2002 and 2005	Van Rensbergen *et al.* (2005), Vandorpe *et al.* (2014)	30 m
Offshore Lanzarote and offshore north Ireland	–	EMONET bathymetry	115 m
Offshore Patagonia (Drake Passage)	–	GEBCO 2021 bathymetry	460 m*

* Due to the relatively low resolution this grid was only used to measure structures above 10 km horizontal distance.

equator. Since the hemisphere is relevant for the directions of the Coriolis force, but not for its strength, the authors have not distinguished between the same latitudes on Northern and Southern Hemisphere.

Bathymetric and seismic data

Bathymetric data were used from nine different areas. Table 1 summarizes the details of where the data comes from and the grid cell size.

The seismic data used in this study for the stratigraphic and morphological analysis of moats was obtained from previously published sources (Table S1). This study also shows unpublished seismic data collected during cruise SO260 onboard the *R/V SONNE* in 2018 (Kasten *et al.*, 2019). Seismic data was acquired during the SO260 cruise with a 225 m (active length) long streamer with 96 channels from University of Bremen, and a SERCEL Mini-GI Gun (Sercel, Nantes, France) with a chamber volume of 2 × 0.24 l as a seismic source. The data processing was conducted with the 'VISTA Desktop Seismic Data Processing Software' (Schlumberger) and included bandpass filtering, de-spiking, common mid-point (CMP) binning, Normal-Moveout (NMO) correction, CMP stacking, noise reduction and finite-difference time migration. 'The Kingdom Software' (IHS Markit) was used for interpretation. To convert the travel time of the seismic waves into depth, a constant velocity of 1500 m/s was used.

Vessel-Mounted – Acoustic Doppler Current Profiler data

For four moats, ocean current velocities were measured with a vessel-mounted Acoustic Doppler Current Profiler (VM-ADCP). These quantitative measurements of the characteristics of ocean currents (strength and direction) at these locations in recent times, but not at times of the moat initiations. Two of the moats are carbonate moats located in the Santaren Channel in the Bahamas, and two are siliciclastic moats located at the open slope offshore north Argentina. The VM-ADCP data from the Argentine moats were partly described by Steinbrink *et al.* (2020) and Wilckens *et al.* (2021), and from the Bahamas moats were partly described in Lüdmann *et al.* (2016). The data from the Bahamas were reprocessed in a similar way as described in Wilckens *et al.* (2021). VM-ADCP

data off Argentina were collected during cruise SO260 between January and February 2018 (Kasten *et al.*, 2019). The instrument parameters led to 16 m depth cells. VM-ADCP data off the Bahamas were collected during cruise M95 between March and April 2013 (Betzler *et al.*, 2014b). The instrument parameters led to 8 m depth cells. Data processing was conducted with the Cascade V7.2 software. For analyses of near-bottom currents, the average speed between 150 m and 200 m above the seafloor was calculated. Data within the deepest 150 m immediately above the seafloor were not used because of their poorer quality due to high scattering from the seafloor. The barotropic tides, obtained from the TPXO tidal model at the time and location of the ADCP acquisition, are below 4 cm/s in the study area and thus much lower than the total current speed. They are not removed from the dataset because they can also transport sediment and meanwhile contribute to total current strength.

Moat names

Several moats are referred to by their previously used name. These names are: Great Bahamas Bank Moat (GBB Moat) and Cay Sal Bank Moat (CSB Moat) in the Bahamas (Betzler *et al.*, 2014a); Ewing Terrace Moat 1 (ET Moat 1) and Ewing Terrace Moat 2 (ET Moat 2) offshore Argentina (Wilckens *et al.*, 2021); Beira Moat offshore Mozambique (Miramontes *et al.*, 2021); Álvarez Cabral Moat in the Gulf of Cadiz (Llave *et al.*, 2001; García *et al.*, 2009); and Gijón Moat offshore northern Spain (Van Rooij *et al.*, 2010; Liu *et al.*, 2020). The moats that have not been previously named are a moat near Madagascar (fig. 3a from Miramontes *et al.*, 2021) that will be referred to here as the Madagascar Moat; a moat near Galicia (fig. 1 from Hanebuth *et al.*, 2015) that will be referred to as the Galicia Moat and a moat near Corsica (fig. 8 from Miramontes *et al.*, 2016) that will be referred to as the Corsica Moat.

RESULTS

Fingerprint of a moat

The moats included in this study are located between 60 m and 5000 m water depth and between latitude 75°N and 67°S. Moat size shows a large variability in terms of width, relief, relief–width ratio, slope angle, drift angle and length (Fig. 3). Relief ranges between 4 m and up to several hundreds of metres like the Madagascar Moat (505 m). Most of the measurements (90%) show a relief below 168 m and the median value is 50 m (Fig. 3; Table 2). Width is between 100 m, and up to tens of kilometres, like the Great Bahamas Bank Moat (26 km). Of all measured moats, 90% are less than 13 km wide, the median width is 2.3 km, and only 10% are <0.5 km wide (Fig. 3; Table 2). Furthermore, the ratio between relief and width varies between 0.001 (for example, Great Bahamas Bank Moat) and 0.1 (for example, Galicia Moat): 90% of all measured relief–width ratios in this study are below 0.056 and the median is 0.022 (Fig. 3; Table 2). Only 10% of the measured moats have relief–width ratios below 0.004. The length of moats is rather difficult to compare since they are often unknown because they are not entirely covered by multibeam data. However, six examples are analysed in section '*Along-slope morphology and hydrodynamics of moat-drift systems*'.

The angle of the slope on which the moats form varies between settings and in particular between open continental slopes and seamounts or other topographic obstacles. In this study, slopes with the highest angles of 25° from the Galicia Moat, located at a topographic obstacle, and 15° at the eastern slope of the Corsica Trough are included (Fig. 3; Table 2). Also, the contourite drift angles vary between settings (see *Methods* for definition). It can be below 1°, for example at the Great Bahamas Bank Moat, but it can also be up to 11°, for example at the Galicia Moat or 10° at the Corsica Moat. However, 90% of the slope angles are below 15° and only 10% are below 1°: 90% of the drift angles are below 8° and only 10% are below 0.4°. The median measured slope angle is 6° and the median drift angle is 3° (Fig. 3; Table 2).

Correlation between parameters of moat-drift systems

In this chapter, the hypothesized correlations between moat relief and width, as well as measured moat parameters and latitude, water depth and steepness of the slope are tested. A comparison between relief and width shows a weak linear trend correlation coefficient (R) of 0.38 (Fig. 4A). The correlation is slightly higher for smaller systems (R = 0.47). Some moat-drift systems, like the Great Bahamas Bank Moat, are up

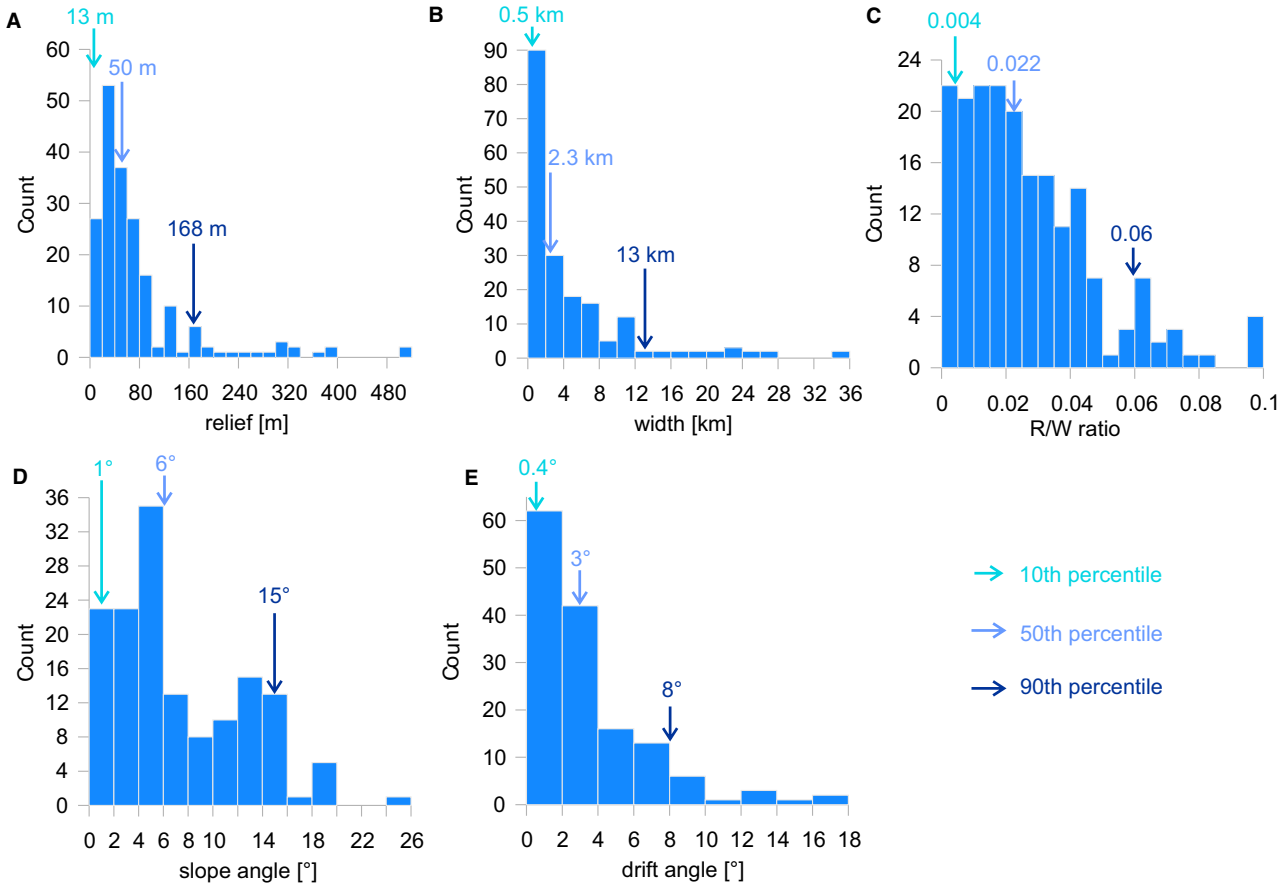

Fig. 3. Histograms showing the range of (A) relief, (B) width, (C) relief–width ratio, (D) slope angle and (E) drift angle.

Table 2. 10th percentile, 50th percentile (median), 90th percentile and maximum from the different measured properties of moats.

	Relief (m)	Width (km)	Relief–Width Ratio	Slope angle	Drift angle
Minimum	4	0.1	0.001	0.3°	0.2°
10th percentile	13	0.5	0.004	1°	0.4°
50th percentile	50	2.3	0.022	6°	3°
90th percentile	168	13	0.060	15°	8°
Maximum	505	35	0.1	25°	17°

to 26 km wide but only have a maximum relief of 54 m, while others, like the Madagascar Moat, have a relief of 505 m but are only 12 km wide. Neither relief, width or relief–width ratio show an apparent correlation with latitude (Fig. 4B to D). A linear fit for relief, width or relief–width ratio against latitude has in all cases a correlation coefficient below 0.16. Moats in deeper water mostly have a higher relief (Fig. 4B). A linear trend is recognized with R = 0.55. However, it has to be noted that shallow moats have a low relief but deep moats can have both a low and a high relief. The width also increases with water depth but this linear trend is weaker with R = 0.2 (Fig. 4F). As a consequence, two linear trends cancel each other out and the relief–

Fig. 4. Diagrams showing correlations between (A) width and relief, (B) relief and latitude, (C) width and latitude, (D) relief–width ratio and latitude, (E) relief and moat water depth (F) width and moat water depth, (G) relief–width ratio and moat water depth, (H) relief and slope angle, (I) width and slope angle and (J) relief–width ratio and slope angle for different latitudes.

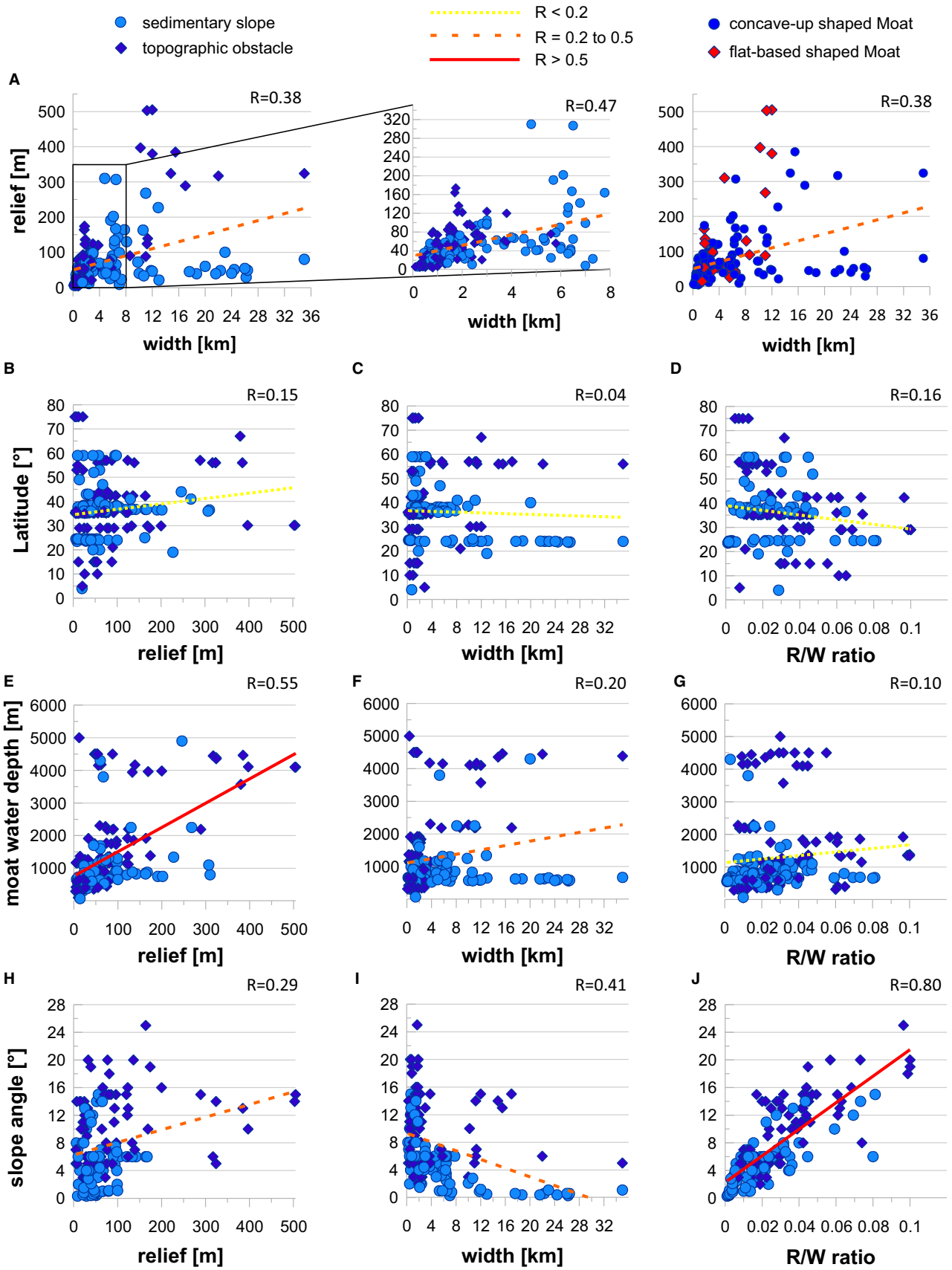

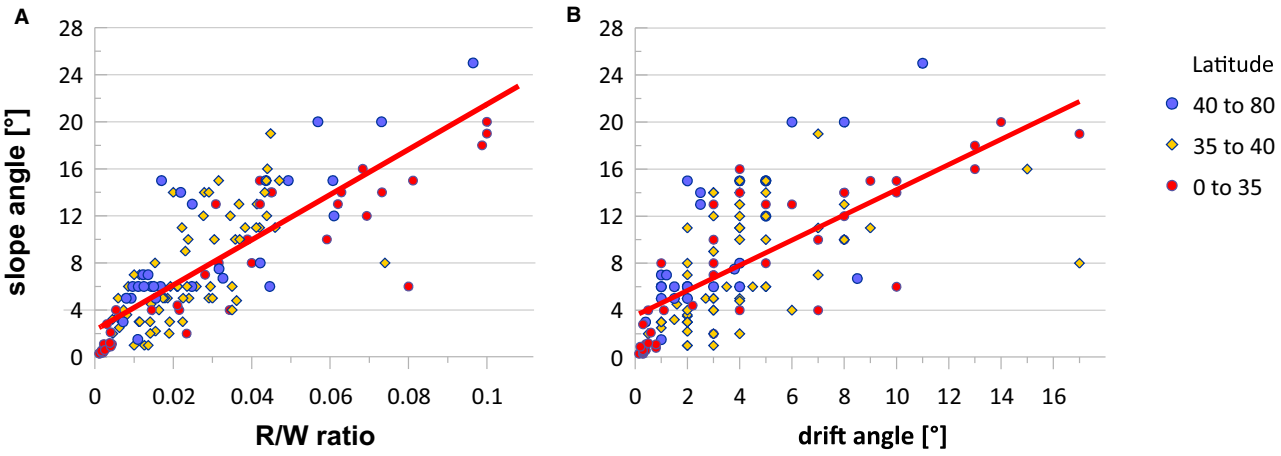

Fig. 5. Diagrams showing correlations between (A) relief–width ratio and slope angle and (B) drift angle and slope angle at different latitudes.

width ratio shows no correlation with water depth (Fig. 4G).

The relief increases and the width decreases with a higher slope angle but the linear trend is only weak with R = 0.29 and R = 0.41 (Fig. 4H and I). As a consequence, there is a high linear correlation between slope angle and relief–width ratio with a correlation coefficient of R = 0.80 (Fig. 4J). Since this correlation is so significant, it might overshadow the possibly small dependence of the moat aspect ratio on latitude. However, a slope angle–aspect ratio diagram with colour-coded latitudes also shows no apparent trend (Fig. 5A). The aspect ratio is influenced by the steepness of the drift angle. Accordingly, moat-drift systems that form at the foot of steep slopes often also have a high angle at the drift side. The angle of the slope side is usually 1.6 times higher than the angle of the drift side (calculated based on the linear fit in Fig. 5B).

Shape and stratigraphy of moat-drift system

Some moats have a moat trough that is flat in cross-section with a very low slope gradient (0–0.5°) and the sides of the moat present a significant and abrupt increase of the slope gradient (2.5–25°). These shapes are here referred to as flat-base shaped, for example the Beira Moat offshore Mozambique or the ET Moat 2 offshore Argentina (Fig. 6A and B). In contrast, in other moats, the slope gradient continuously decreases until the deepest point of the moat and these moats do not present a flat thalweg in cross-sections (slope angle >0.5°). These shapes are here referred to as concave-up shaped. Concave-up shaped moats are for example the Álvarez Cabral Moat or the Gijón Moat offshore Spain (Fig. 6C and D). Of all measured moat cross-sections, 80% are concave-up shaped. The shape of the cross-section can change along a moat. For a more detailed comparison (in addition to the relief and the width at the top of the moat) the width in the middle of the moat was also measured, and for flat-base shaped moats the width at the bottom of the moat was measured (Fig. 6). A comparison between flat-base and concave-up shaped moats indicates that the shape does not significantly depend on the width or relief of the moat (Figs 4A and 6). The aspect ratio of flat-base shaped moats is on average 6% higher than from concave-up shaped moats.

The stratigraphy of analysed moats differs in the following ways: (i) some reveal aggrading patterns; (ii) some only migrate laterally; and (iii) some are more erosive. Examples of the first type showing an aggrading pattern are the Beira moat-drift system and the Gijón moat-drift system (Fig. 6A and B). The seismic reflections follow the moat morphology and onlap at the slope side. These are defined here as 'Constructional Moats'. An example of the second type with lateral migration is the ET moat-drift system 2 (Fig. 6B). Going from drift to moat, the slope angle of the seismic reflections increases and reflections downlap at the bottom of the moat. These are defined here as 'Mixed Moats'. An example of the third type that shows more erosion is the

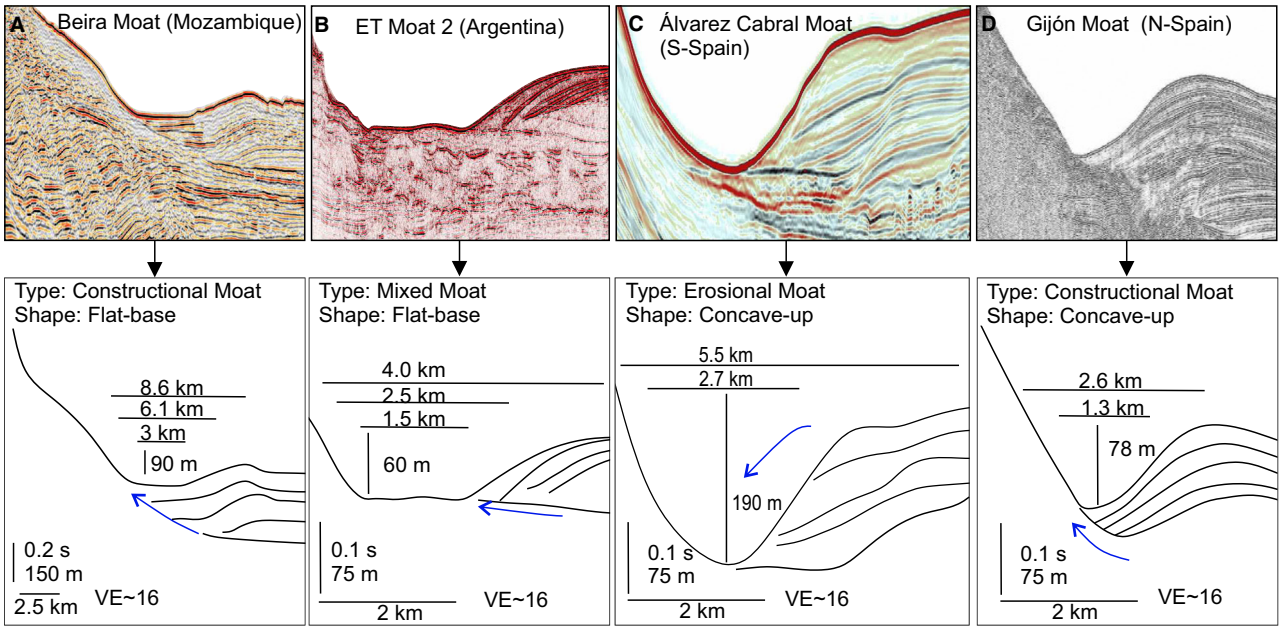

Fig. 6. Stratigraphy with a Vertical Exaggeration (VE) of 16 of: (A) the Beira Moat (adapted from Thiéblemont *et al.*, 2019; Miramontes *et al.*, 2021); (B) the ET Moat 2; (C) the Álvarez Cabral Moat (adapted from Hernández-Molina *et al.*, 2016); and (D) the Gijón Moat (adapted from Liu *et al.*, 2020). The moats show examples of flat-base and concave-up shaped moats as well as three different stratigraphic types. The blue arrow indicates the migration direction of the moat.

Álvarez Cabral moat-drift system (Fig. 6C). Here, seismic reflections are truncated at the drift side and show only a slight dip towards the moat. These are here defined as 'Erosional Moats'. It is possible that some cross-sections from the same moat show an Erosional Moat while others show a Constructional Moat. Additionally, moats may evolve with time from one type of moat to another. This is for example the case for the Álvarez Cabral Moat or the ET Moat 2. A comparison between different internal architectures of 40 classified moat cross-sections indicates that the stratigraphic differences do not depend on the width or relief of the moat. From all (40) classified moat cross-sections in this study 78% are Constructional Moats, 15% are Mixed Moats and only 8% are Erosional Moats.

Along-slope morphology and hydrodynamics of moat-drift systems

Bathymetry

Moats located in six different settings, covering a wide range of typical geological and hydrodynamic settings, are further analysed not only in across-slope direction, but also in along-slope direction (Figs 7 and 8). Two moats are located in the Bahamas, two at the Argentine continental margin, one west of Corsica and one offshore Galicia. Two over 100 km long moats from the Santaren Channel in the Bahamas are chosen (Fig. 7B). Here, the current flows northward along the Great Bahamas Bank forming the Great Bahamas Bank Moat (GBB Moat) and southward along the Cay Sal Bank forming the Cay Sal Bank Moat (CSB Moat). The drift in the Santaren Channel (Bahamas) can be classified as a confined drift, due to the mounded drift morphology in the centre of the channel and the two moats on the flanks (Paulat *et al.*, 2019). However, here the confined drift will simply be referred to as two separated mounded drifts that have grown into one another but are still associated with two moats (Fig. 7B). The eastern half of the confined drift, which is close to the GBB, is the drift that is associated with the GBB Moat, and the western half of the confined drift is associated with the CSB Moat (Fig. 9). Two over 80 km long moats called Ewing Terrace Moat 1 (ET Moat 1) and Ewing Terrace Moat 2 (ET Moat 1) from the Argentine continental margin are found where the Malvinas current flows

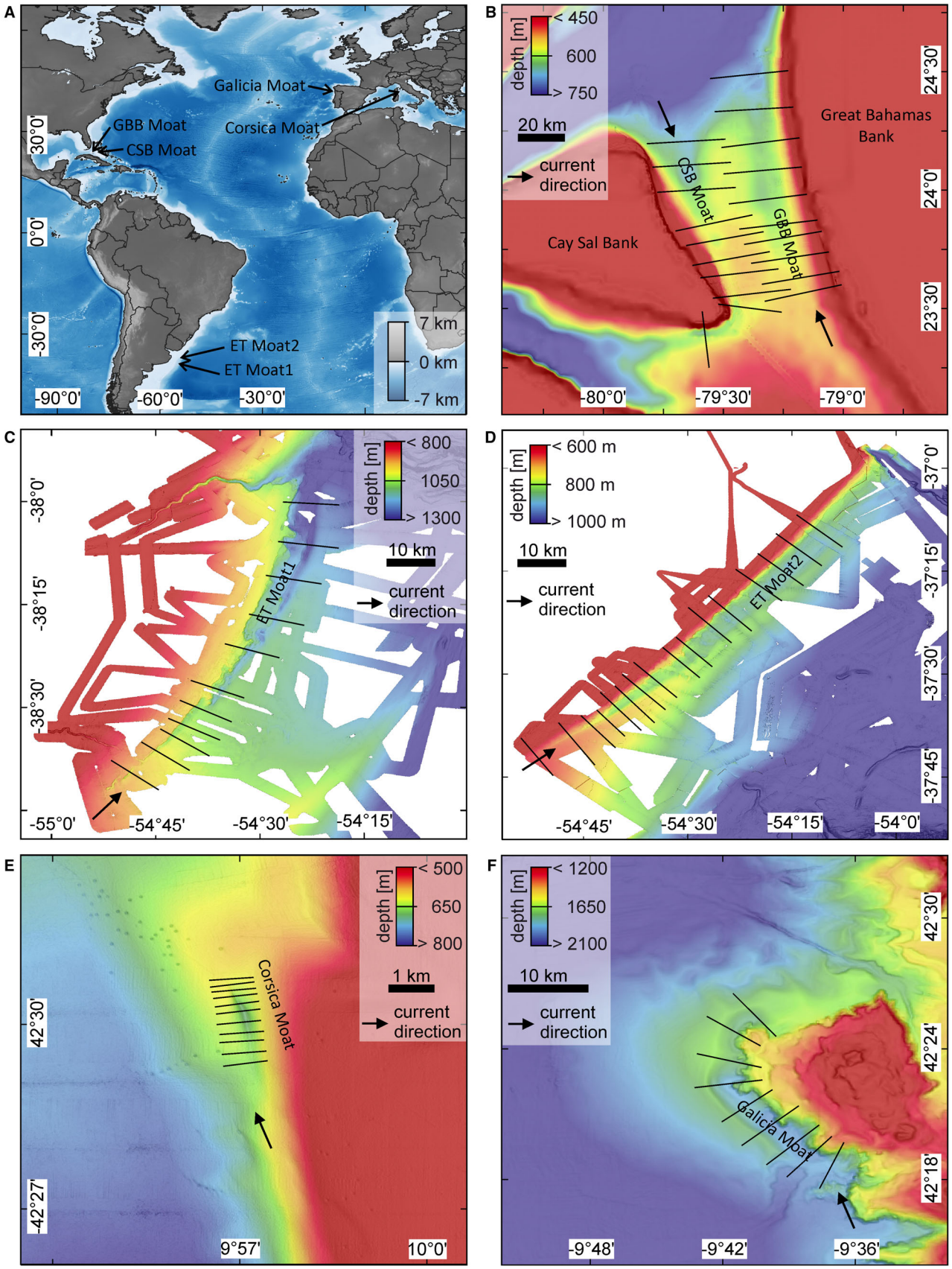

Fig. 7. Bathymetry of six different moats. (A) Overview map showing location of moats. (B) Santaren Channel in the Bahamas with the GBB Moat (Great Bahamas Bank Moat) and the CSB Moat (Cay Sal Bank Moat). (C) ET Moat 1: Ewing Terrace Moat 1 and (D) ET Moat 2: Ewing Terrace Moat 2 offshore north Argentina. (E) Corsica Moat east of Corsica. (F) Galicia Moat at the foot of a topographic obstacle offshore Galicia. The black lines indicate the position of the measured topographic profiles.

northward (Fig. 7C and D). The moat west of Corsica is, with only 2.8 km in length, much smaller than the other five moats and forms in a zone of northward current flow (Fig. 7E). The 17 km long moat offshore Galicia represents one example of a moat that formed at the foot of a topographical obstacle, where the current flows northward (Fig. 7E). For the six moats which were analysed in detail, the current main flow direction is known from previous studies (references listed in Table S1).

The moats are here always analysed in a downstream direction (Fig. 8). Moat and drift depth can become deeper (GBB Moat, ET Moats) or shallower (Corsica and Galicia Moats) in the downstream direction (Figs 7 and 8). Comparing the moat depth with the drift crest depth shows that the relief is sometimes caused by a drastic deepening of the moat rather than the growing of a significant mounded drift. This is most significant for the Corsica Moat and is also observed in the ET Moat 2 at 10 to 20 km along-slope distance (Fig. 8D and E), demonstrating that the separated mounded drifts that are identified in the seismic cross-sections do not always show a pronounced mounded shape in the bathymetry in the along-slope direction. Only the GBB drift shows a slight mounded shape at the beginning at approximately 0 to 20 km distance (Fig. 8A). The straight moats at the open slope of the Argentine margin are widening in the downstream direction (Figs 7C, 7D, 8C and 8D). However, the CSB Moat becomes narrower and the GBB moat first widens and then gets narrower (Fig. 8A and B). The Galicia moat, located at the topographic obstacle, shows no clear trend regarding the width (Fig. 8F). The relief–width ratio curve always shows a similar trend as the relief curve. Generally, the relief–width ratio at the very gentle slopes of GBB Moat and CSB Moat is two orders of magnitude lower compared to the steeper slopes of the Corsica Moat or the Galicia Moat (Fig. 8). When the slope angle becomes steeper, the drift angle usually shows the same trend. At the Corsica Moat, where the slope angle smoothly but significantly increases from 8° to 15°, the drift is following the same trend but with slightly lower values (2° to 9°). While the slope angle starts decreasing again at a distance of 1.8 km, the drift angle only starts decreasing at 2.2 km distance (Fig. 8E).

Current measurements

The VM-ADCP data close to the seafloor generally shows stronger currents above the ET Moat 1, ET Moat 2, GBB Moat and CSB Moat compared to the speed above the associated separated mounded drift (Table 3). For the moats offshore Argentina (Southern Hemisphere; therefore the current is pushed towards the left by the Coriolis force), the difference in the mean near-bottom speed above the moat and above the drift is 9 cm/s (32%) for the ET Moat 1 and 14 cm/s (48%) for the ET Moat 2. For the GBB Moat, the near-bottom speed difference between moat and drift is slightly lower with 7 cm/s (20%) and for the CSB Moat the difference is small with only 1 cm/s (5%).

The ADCP data from the Bahamas (Northern Hemisphere; therefore the current is pushed towards the right by the Coriolis force) shows that the current flowing northward becomes more focused on the right boundary (the slope of the GBB) in a downstream direction. At the first cross-section located at the southern side of the Santaren channel, the highest speed is situated in the middle of the channel and at the slope of the GBB (Fig. 10A and C). A second cross-section, located further to the north shows higher speeds near the GBB (Fig. 10B and D).

DISCUSSION

Classification of deep-sea elongated depressions

Different nomenclatures have been used for the elongated depressions that are formed by bottom currents. Faugères *et al.* (1999) introduced the terms ‘moat channels’ and ‘drift levées’. Later

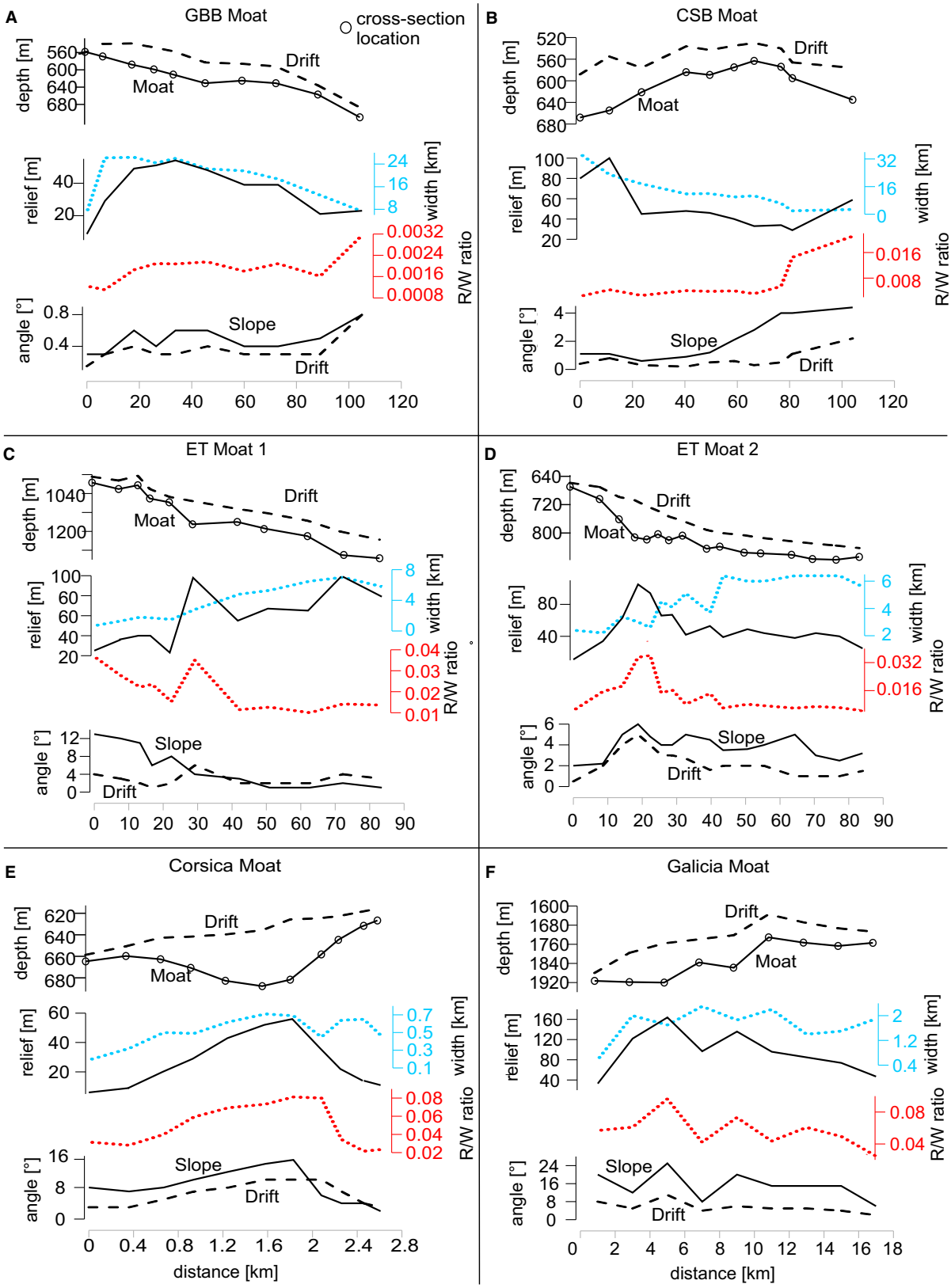

Fig. 8. Along-slope measurements of six different moats: (A) GBB Moat – Great Bahamas Bank Moat; (B) CSB Moat – Cay Sal Bank Moat; (C) ET Moat 1 – Ewing Terrace Moat 1; (D) ET Moat 2 – Ewing Terrace Moat 2; (E) Corsica Moat; and (F) Galicia Moat. R/W ratio stands for relief–width ratio. See Fig. 7 for location.

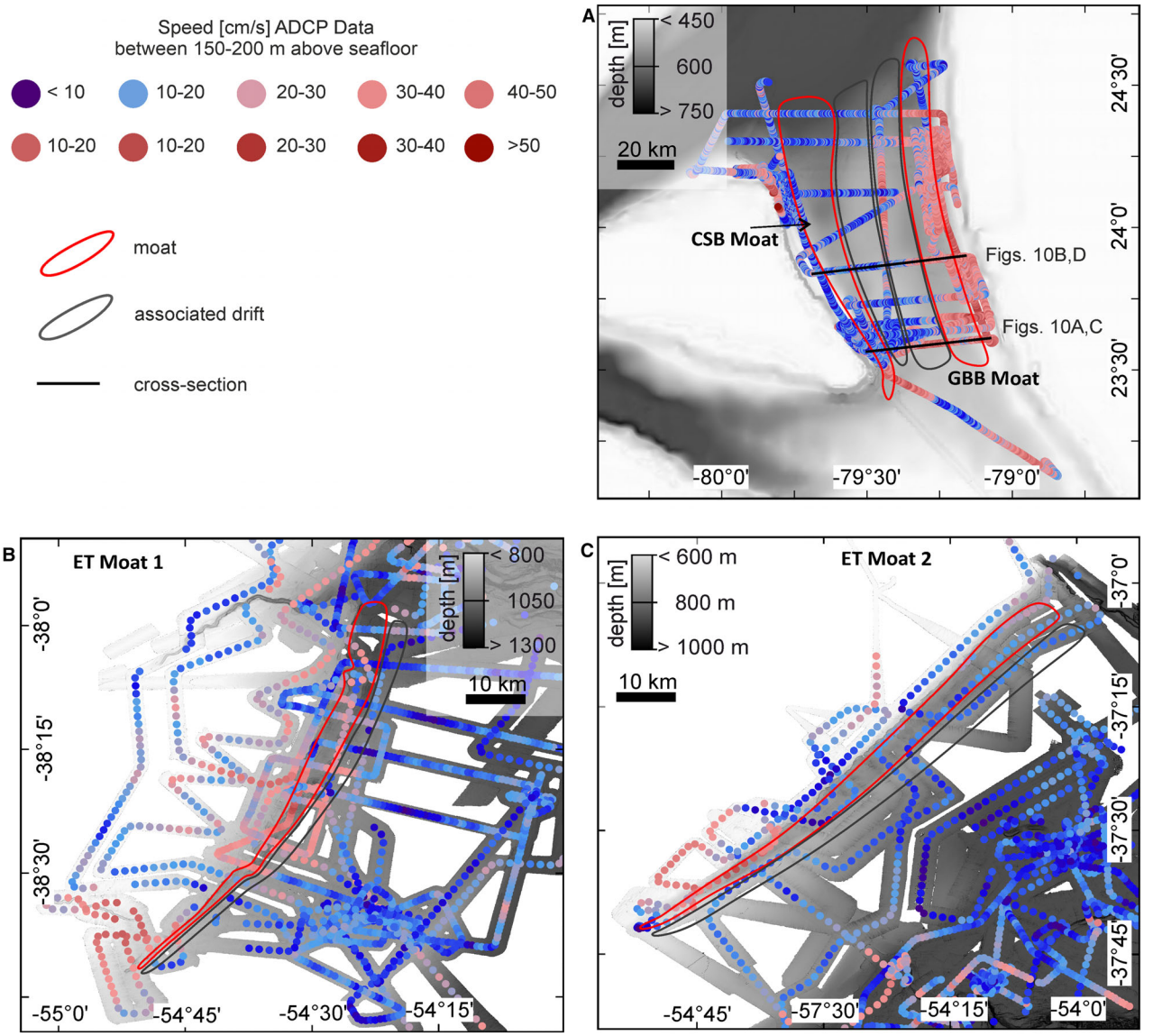

Fig. 9. Vessel-mounted Acoustic Doppler Current Profiler (VM-ADCP) data averaged between 150 to 200 m above seafloor from: (A) GBB Moat – Great Bahamas Bank Moat, and CSB Moat – Cay Sal Bank Moat; (B) ET Moat 1 – Ewing Terrace Moat 1; and (C) ET Moat 2 – Ewing Terrace Moat 2.

Table 3. Mean speed at 150 to 200 m above the seafloor, as well as the standard deviation and maximal speed above the moats and above the associated drifts. CSB Moat, Cay Sal Bank Moat; ET Moat 1, Ewing Terrace Moat 1; ET Moat 2, Ewing Terrace Moat 2; GBB Moat, Great Bahamas Bank Moat.

	Moat speed (cm/s)			Drift speed (cm/s)			
	Mean speed	Standard deviation	Maximum speed	Mean speed	Standard deviation	Maximum speed	Difference in mean speed between moat and drift (%)
ET Moat 1	28	11	51	19	10	36	32
ET Moat 2	29	17	63	15	6	39	48
GBB Moat	35	13	87	28	14	72	20
CSB Moat	20	14	68	19	11	61	5

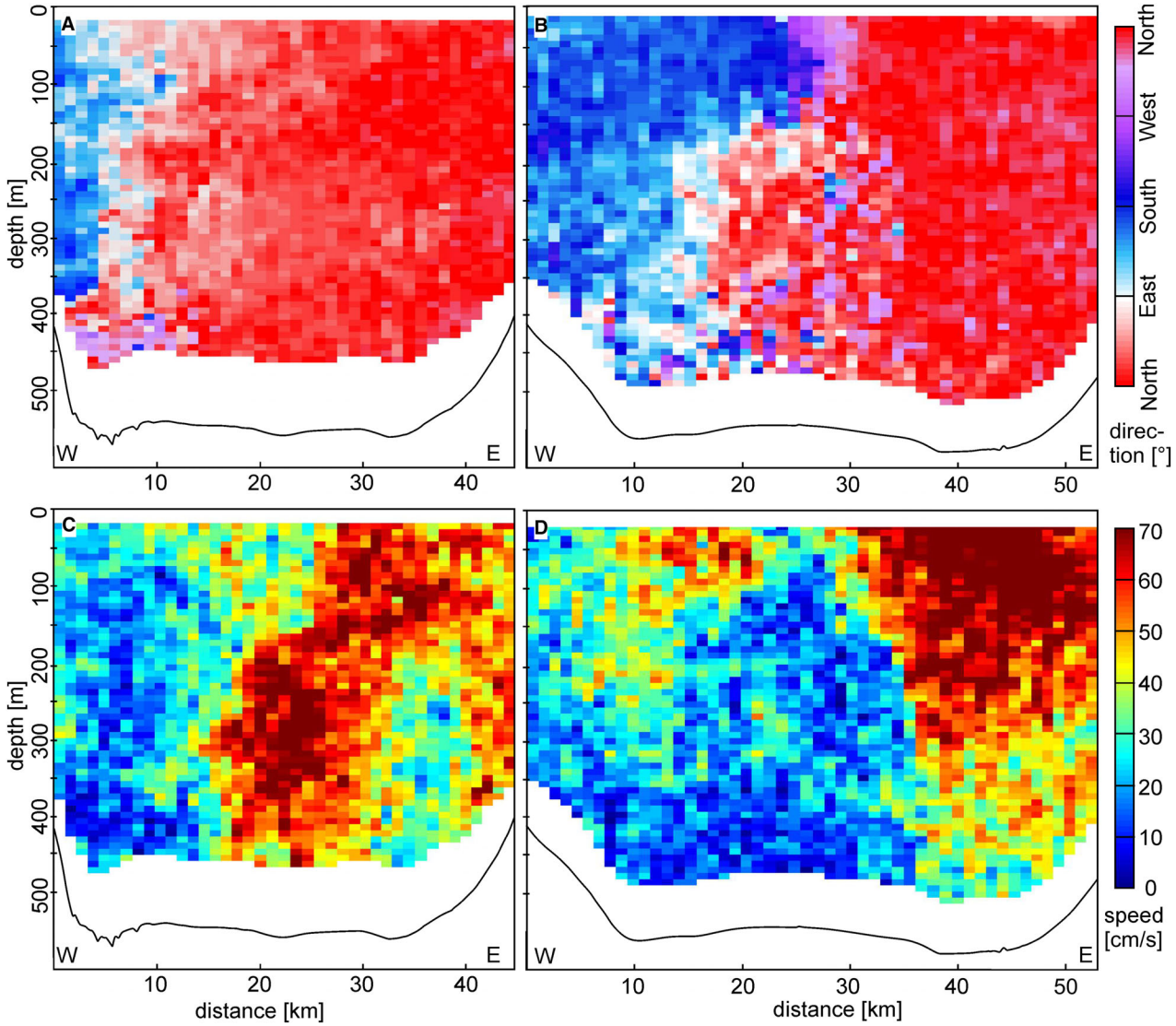

Fig. 10. Cross-section of the Bahamas showing the measured flow direction at (A) southern part of the channel and (B) middle part of the channel and the measured flow speed at (C) southern part of the channel and (D) middle part of the channel. See Fig. 9 for location.

the terms 'moat' and 'separated elongated mounded drift' were widely established (Rebesco, 2005; Rebesco *et al.*, 2014). From the stratigraphic analysis herein, the authors suggest to subclassify three different main types of moats that can be distinguished based on the termination location of the drift reflections. For the first moat stratigraphic type, reflections onlap at the slope side (Fig. 11A). They are classified as 'Constructional Moats' because they present an aggrading stacking pattern in the moat. This moat-drift system can also migrate up-slope. At this type of moat, the separated mounded drift has a pronounced drift crest (Betzler *et al.*, 2014a; Zhao *et al.*, 2015; Miramontes *et al.*, 2016; Yin *et al.*, 2019). However, the form of the drift crest is affected by the pre-existing morphology. For example, the drifts associated with a moat that form at a pre-existing slope will have a more pronounced drift crest (Miramontes *et al.*, 2016) than the associated drifts that form on a flat surface, such as a terrace or the basin floor (Miramontes *et al.*, 2019; Wilckens *et al.*, 2021). For the second moat stratigraphic type, reflections downlap at the bottom of the moat (Fig. 11B). They are classified as

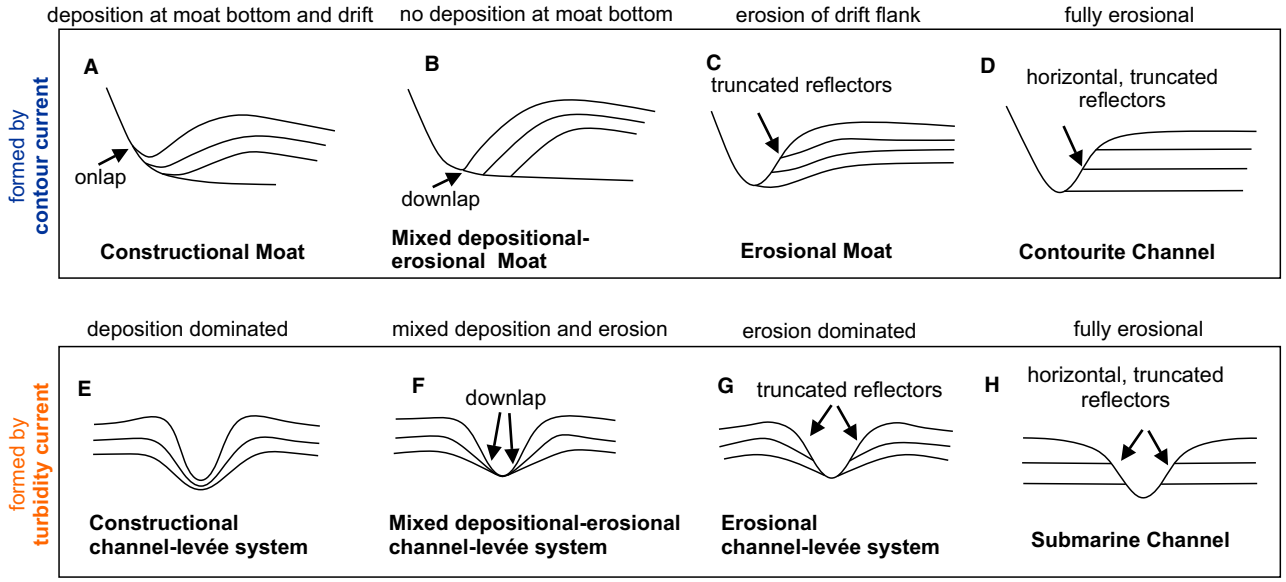

Fig. 11. Nomenclature of elongated depressions in the deep sea based on seismic or sub-bottom profiler data. Three different stratigraphic types of moats: (A) *Constructional Moat* – reflections onlap at the slope side; (B) *Mixed Moat* – reflections downlap at the bottom of the moat; (C) *Erosional Moat* – reflections are truncated at the drift side. (D) Similar to moats contourite channel are also formed due to contour currents, but they are more erosive and no pronounced drift crest is present. Three different stratigraphy types of levéed submarine channels (channel-levée systems) formed by gravity flows: (E) constructional channel-levée system, (F) mixed depositional – erosional channel-levée system, (G) erosional channel-levée system, (H) Submarine channel with no levées (adapted from Stow & Mayall, 2000, Mulder, 2011).

'Mixed depositional – erosional Moats' or in short 'Mixed Moats' because almost the same amount of sediment that is eroded is also deposited at the bottom of the moat (no erosion and no deposition occurs on average). Accumulation dominantly occurs at the drift alongside the moat. This moat-drift system mainly migrates laterally and does not show vertical aggradation at the moat trough. At the third moat stratigraphic type, reflections are truncated at the drift side (Fig. 11A). They are classified as 'Erosional Moats' because erosion is the dominant factor shaping the moat morphology. Here, no pronounced drift crest is present (Hernández-Molina *et al.*, 2016; Miramontes *et al.*, 2021). It is possible that a moat transitions with time and/or in downstream direction into another moat type. Moats occur at erosive slopes (Hernández-Molina *et al.*, 2016; Wilckens *et al.*, 2021) and non-erosive slopes (Wunsch *et al.*, 2017).

Previously, moats have often been described as erosive or non-depositional features (Hernández-Molina *et al.*, 2006, 2008; Ercilla *et al.*, 2016; Yin *et al.*, 2019; Miramontes *et al.*, 2021; Chen *et al.*, 2022). Miramontes *et al.* (2019) suggested that during energetic periods the sediment inside moats is eroded. During less energetic periods, the sediment can be deposited inside the moat. The balance between erosion and deposition determines the stratigraphy. This study shows that not all moats are erosive or non-depositional features. In fact, most moats (78%) considered in this study are Constructional Moats, which means that sediment is not only accumulated at the drift alongside the moat but also at the bottom of the moat. Based on these results it is hypothesized that, on average, most moats at present day are not erosive but rather formed by differential sedimentation; i.e. less sediment is deposited inside the moat compared to the separated elongated mounded drift alongside the moat.

Both moats and contourite channels are formed by contour currents. The elongated depression is defined as a moat when the drift reflections bend towards the deepest point of the moat (Fig. 11A to C). Alongside contourite channels no drift is formed and, thus, no drift crest is present (Miramontes *et al.*, 2021). Sometimes also other oceanic processes can form elongated depressions; this includes for example internal waves that

propagate at density boundaries within the water column (Miramontes *et al.*, 2020); or several pockmarks that were formed by fluid seepage and then get eroded and thus elongated by bottom currents (Yu *et al.*, 2021). These channels do not form alongside a slope break or an escarpment, but they occur on the slope without any topographic constraints. Similar to ocean driven currents, downslope flowing turbidity currents can also form elongated depressions that are called submarine channels, and if sediment is overspilled at the channel walls, they form levées and are classified as channel-levée systems (Clark *et al.*, 1992; Hiscott *et al.*, 1997; Peakall *et al.*, 2000; Deptuck & Sylvester, 2018). The channel forming a channel-levée system is here named submarine channel because it develops due to gravity driven flows (Clark *et al.*, 1992; Hiscott *et al.*, 1997; Peakall *et al.*, 2000; Deptuck & Sylvester, 2018). They are subclassified into constructional (or depositional), mixed and erosional channel-levée systems based on the balance between deposition and erosion (Imran *et al.*, 1998; Stow & Mayall, 2000; Mulder, 2011). Submarine channels that do not have associated levées are fully erosive submarine channels (Fig. 11H) similar to contourite channels that do not have an associated drift (Fig. 11D). Our suggested nomenclature for the contour-current formed moats is adapted from the established subclassification for channel-levée systems and submarine channels (Stow & Mayall, 2000; Mulder, 2011) (Fig. 11E to H). The resembling nomenclature defines comparable stacking patterns observed in moats and submarine channels, despite the fact that the physical drivers behind the oceanographic and turbidity currents are different. In both cases, the current primarily transports sediment along the moat or channel and deposition rates are highest in the associated drift or levées.

Moat and contourite drift location

Moats are observed in many different settings distributed over the entire world's oceans and in lakes. However, regional studies show that moats are not observed at all slopes of contourite depositional systems (e.g. Miramontes *et al.*, 2021; Wilckens *et al.*, 2021). Thus, there must be additional factors that determine whether a moat can form at a specific location. One of these factors is the Coriolis force, which influences ocean circulation. On continental margins, moats can form where the Coriolis force is steering the current towards the slope (Faugères *et al.*, 1999; Llave *et al.*, 2001; Rebesco *et al.*, 2014). Moats can be located in tectonically active areas like the Gulf of Cadiz (Llave *et al.*, 2001; García *et al.*, 2009), the Aegean Sea (Tripsanas *et al.*, 2016) or offshore north-west New Zealand (Steinbrink *et al.*, 2020; Bailey *et al.*, 2021). However, none of the moats analysed in this study are from a subduction zone (Fig. 1). One small moat is reported at the active area of the North Scotia Ridge (Nicholson *et al.*, 2020). Active margins are shorter, steeper and contain 15% more canyons than passive margins, and include shorter, steeper and more closely spaced submarine channels than passive margins (Harris & Whiteway, 2011). Furthermore, earthquakes that can trigger mass movements are common at active margins. Therefore, downslope processes occur more frequently at active margins and probably tend to overprint most moats. This might also be the case for Contourite Depositional Systems (CDSs) in general, which are predominant at passive margins (Rebesco *et al.*, 2014). The failure that can be triggered by earthquakes and leads to a mass-wasting event is more likely to occur in contourites, particularly in plastered drifts, rather than hemipelagic sediment due to the convex geometry with steep slopes, but both types of sediments have similar mechanical properties (Miramontes *et al.*, 2018). Nicholson *et al.* (2020) suggested that large drifts do also occur at active margins but are reshaped by downslope processes, which makes it difficult to identify them. In summary, only a few studies on contourites have been performed in active margins, but bottom currents also influence them. The resulting morphologies are often cannibalized by subduction processes, destroyed by tectonic processes, or removed or reworked by gravity-driven processes. This is likely the reason why along active margins a CDS cannot always be established, or current-related features are smaller because they are constrained to small-scale obstacles. More work is needed to understand the influence of bottom currents on active margins and to determine the moat-drift morphologies in these areas.

Moats are not only located along continental margins but also form around seamounts or other obstacles (for example, cold-water coral mounds) in the ocean. Forcing from topographic barriers that can focus and intensify the current might also be involved in the moat formation. Examples are the Madagascar seamount moats

(Miramontes *et al.*, 2021) or a moat in the Mediterranean Sea (Llave *et al.*, 2020). In the case of the Madagascar moat, the current is flowing through two seamounts (Miramontes *et al.*, 2021) and in the case of the Mediterranean Sea moat, it is flowing through the Alboran Trough (Llave *et al.*, 2020). These moats are often restricted to a relatively small area depending on the size of the topographic obstacle. At the Madagascar seamount, with a *ca* 20 km diameter, the moats are less than 25 km long. Around this large seamount two distinct moats form at each side, while around smaller seamounts (for example, in the Gulf of Cadiz, with seamounts <5 km in diameter), moats form all around the seamounts. The dimension of the seamount, the strength of the current and the latitude jointly influence sedimentation around seamount (Zhang *et al.*, 2016). Additionally, moats that develop all around the seamounts might be linked to changes in current direction (for example, driven by tides, mesoscale eddies). Without long-term current measurements or numerical modelling, it is difficult to conclude which process is dominant. At three seamounts in the Gulf of Cadiz, the moat closest to the shelf is wider and has a larger relief, while the moat that is on the side towards the basin is narrower and has a smaller relief. The uneven moat-drift system size might be related to more sediment being available on the landward side of the seamount. Aspect ratio and drift angle are not affected by this. Previously, the uneven size of moats at seamounts was linked to the Coriolis force pushing the current towards one of the seamount's sides, which intensifies the current and leads to more erosion compared to the other side (Hernández-Molina *et al.*, 2006; Chen *et al.*, 2022). However, both effects can explain all of the here discussed examples and thus further data is needed to determine which process is dominant.

Factors influencing the moat and drift formation

Moats are formed by ocean currents, thus the information about the ocean current direction and speed that formed the moat and associated drift should be recorded in the morphology and stratigraphy. Untangling this information from other factors that affect moat development will only become possible after gaining a better understanding of what factors significantly influence moat development. The four moats considered in this study with ADCP data available show that the speed above the moats is higher compared to areas above the drift. This could mean that due to the higher transport capacity of strong currents more sediment is transported through the moats compared to the surrounding area. This suggests that moats also play an important role in sediment transport. These observations suggest that neither shape nor stratigraphic type depend only on the size of the moat. Furthermore, there is a wide range of aspect ratios for moats (Fig. 4A) and thus current speed alone cannot explain the development of moat-drift systems. Presumably, the development of moats is influenced by: (i) the steepness of the slope; (ii) the geological and oceanographic setting; (iii) the current velocity and velocity changes in time and space, and the Coriolis force and Rossby number; and (iv) sediment type and the amount of sediment that is transported by the currents. Furthermore, the influence of downslope transported sediment (Vandorpe *et al.*, 2014; Betzler *et al.*, 2014a) that can be deposited inside the moats, like turbidites or mass transport deposits, should also be considered. An additional influence on moat shape can come from syn-sedimentary faults in the moat-drift system (Hernández-Molina *et al.*, 2016) or local eddies (Wilckens *et al.*, 2021). Moats might also be influenced by internal waves propagating at density boundaries or by surface fronts in the ocean (Hernández-Molina *et al.*, 2008; Nicholson & Stow, 2019). Furthermore, the statistical analyses of moat-drift systems confirm our hypothesis that moat morphology correlates with water depth. This might be because of the influence of sediment availability and limited accommodation space.

1 The statistical analyses indicate that the aspect ratio of moats correlates with the slope angle of the slope where the moat forms. More precisely, the steeper the slope, the larger the aspect ratio and the higher the drift angle. Thus, the authors suggest that the slope angle locally influences the along-slope current dynamics by affecting the across-slope velocity gradient and this controls the aspect ratio of moats. This correlation is not only shown by the analyses of 185 cross-sections, but also in the along-slope analyses of moats. Usually, when the slope angle changes in the downstream direction, the aspect ratio also changes. While the current flows along the slope, it needs time to adapt to changes in the slope. Thus, the adaptation in aspect ratio can only occur a couple of

kilometres downstream (Fig. 7E). The amount of downslope transported sediment can affect the aspect ratio of moats but apparently this is usually not so significant that it overprints the effect of the slope angle on the moat development.

2 To further understand moat development, it is necessary to distinguish between three different environments: open slope, channel and topographic obstacle (Fig. 12). Moats can form at an open slope that is mainly affected by a current (for example, Argentine margin). At the Argentine margin, the moats are widening in a downstream direction. This might also be common at other open slopes but currently there is not enough data available to support and generalize this observation. Moats can form inside a channel with currents flowing in different directions (for example, the Santaren Channel). Here, the shape of the drift is possibly related to the strength difference of the two currents. In the case of the Santaren Channel, the drift bends in the same way as the slope of the Great Bahamas Bank. This indicates that the northward flowing current that creates the Great Bahamas Bank moat is the strongest current and mainly responsible for the drift morphology. The VM-ADCP data also shows that the northward flowing current is stronger compared to the southward flowing current. At the southern side, the drift is very flat and not very mounded (Lüdmann *et al.*, 2016). This indicates that the flow is not yet adapted to the morphological changes, and it is thus not in equilibrium with the morphology. Downstream, the current becomes more focused, and the drift gets more mounded (Fig. 10). The morphology can also be correlated with the discharge or volumetric flow rate of water depending on the speed of the current and the area of the cross-section through which the water can flow. As described by the continuity equation, this means that within one moat, the current velocity changes if the area of the cross-section changes. This link was shown for the moats in the Santaren Channel and the morphological evolution could also be linked to the Gulf Stream that flows through the Florida Strait north of the study area (Paulat *et al.*, 2019). Moats can also form around topographic obstacles. Here, the current has to adapt constantly to the changes in slope and thus is never in equilibrium with the morphology.

3 The importance of the Coriolis force in moat formation has been previously suggested (Faugères *et al.*, 1999). Even though the Coriolis force strength depends on the latitude, there is no statistical correlation between latitude and size or aspect ratio of moat. Moats in very low latitudes (<20°) are in the presented analyses narrower and have a smaller relief than moats in higher latitudes (>20°). However, this is statistically not significant and should be further tested by numerical modelling. The Coriolis force also depends on the current speed, which is rarely known for moats and thus cannot be included in the present analyses. The Rossby number (Ro = U/fL) is used to determine how important the Coriolis force is in a system (Davarpanah Jazi *et al.*, 2020). The ADCP current speed measurements in this analysis show that the average speed above the moat is approximately U = 0.25 m/s and the average moat width is 2300 m. Assuming that the average moat is at mid-latitudes (45° North or South) then the Coriolis frequency is f = 10e−4 rad/s and, together with the average moat width and average speed above moats, the Rossby number is 1. A small (<1) Rossby number indicates that the system is significantly influenced by the Coriolis force (Wells & Cossu, 2013). Contour currents that are in a geostrophic balance have, by definition, a Rossby number of Ro = 1. Thus, the Coriolis force should play a role in moat development and moats should thus scale as $L \sim Uf$. However, the data do not show a statistical dependence of moat parameters on the latitude, which indicates that other factors like the steepness of the slope at which the moat forms or current speed are so dominant that a small dependence on the Coriolis frequency cannot be recognized. New ADCP data can be used to properly scale the current flowing through the moat, similar to

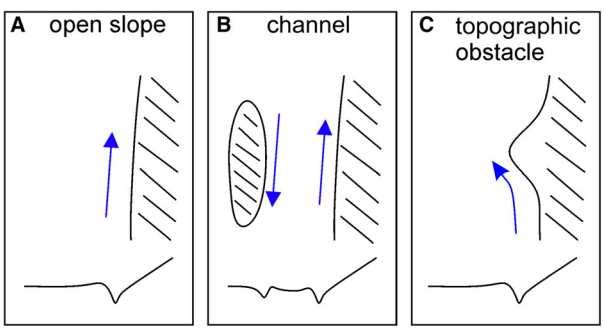

Fig. 12. Sketches showing in plan view the main settings where moats form. Moats can form at an open slope that is affected by a current, they can form in a channel with currents flowing in different directions and they can form around topographic obstacles. Blue arrows indicate flow direction.

previous work about buoyant gravity currents (Lentz & Helfrich, 2002). As a next step, a multivariate analysis that includes current speed measurements inside and adjacent to moats is necessary to better understand how the Coriolis force affects moat development.

4 The slope angle only affects the aspect ratio, but the size and type of the moat is not constrained by the slope angle alone. Also, in the slope angle versus aspect ratio plot (Fig. 4J), some scattering of data points around a linear curve was found. Thus, other factors like current velocity and velocity gradient must be considered. The authors suggest that the size of the moat is controlled by the current speed and the horizontal velocity gradient (Fig. 13). Based on the ADCP current measurements, the bottom current is above 10 cm/s and below 1 m/s, but the exact value cannot be given due to the limited current measurements above moats. For a moat to be formed, higher speeds must exist over the moat and lower speeds over the drift. One factor that influences this velocity gradient is the slope angle. Based on the combined results herein, a new moat formation concept is introduced that depends on current speed and slope angle. So far this is only a qualitative concept. It is suggested that a current with low speeds (exact current speed depends on seafloor sediment grain size and composition) at a gentle slope will not create a moat; while the same current at a steeper slope could create a moat. A fast current at a gentle slope can create a wide moat with a low aspect ratio (for example, GBB moat); while the same current at a steeper slope would create a narrower moat with a higher aspect ratio. The slope angle is only one factor influencing the vertical speed gradient, another factor might be the interaction of two currents with one another. One example is the interaction of the two currents in the Santaren Channel flowing in opposite directions.

5 Sediment supply and sediment type are most likely another important parameter influencing the moat-drift system stratigraphy. The thickness of all constructional contouritic elements including Constructional Moats and the associated drift must depend on the sediment availability and current speed. Erosional features or non-depositional features must be connected to the absence of sediment availability and/or high bottom current speeds that allow only bypassing of the sediment. However, this study could not quantify this effect. Possibly sediment

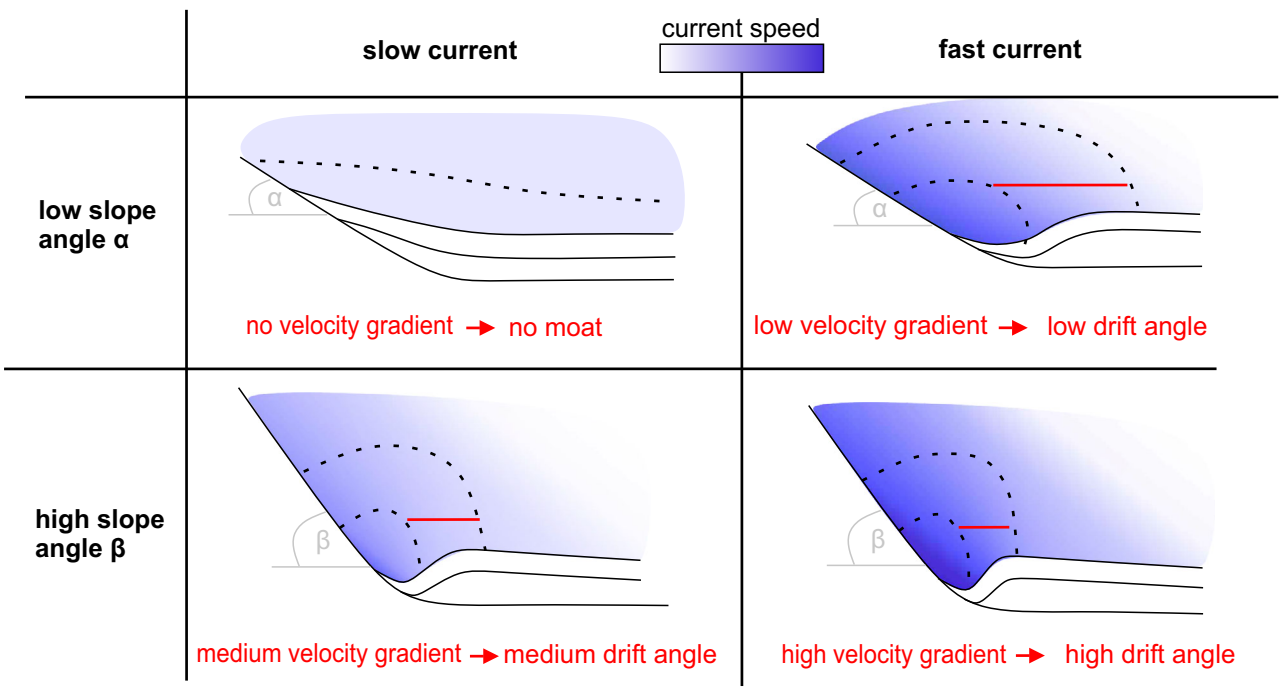

Fig. 13. Conceptual model of how moats form under different slope angles and current velocities. Slope angles and current velocities together influence the current velocity gradient. The current velocity gradient then determines the drift angle and thus the shape of the moat.

consolidation and sediment composition can affect whether a moat becomes more flat-base or concave-up shaped.

For future studies, the authors suggest using moorings with ADCPs and sediment traps to further analyse the sediment transport and other possible oceanographic secondary processes such as internal waves, tides and vortices/eddies in moats.

CONCLUSIONS

This study provides a general comparison of 185 cross-sections from moat-drift systems distributed in 39 different parts of the oceans and lakes, as well as a detailed analysis of six moat-drift systems that cover a wide range of typical geological and hydrodynamic settings. Additionally, measured current data from four moats were analysed to better understand the hydrodynamics. This allows the authors to propose a general conceptual model of moat-drift system morphology and stratigraphy and suggest what parameters influence their development. The conclusions can be summarized as follows:

- Based on the measurements of 185 cross-sections, the parameters that are common for moats were determined. The median moat cross-section has a 50 m relief, 2.3 width, 0.022 relief–width ratio, 6° slope angle and 3° drift angle.
- Three main types of moat can be distinguished based on their stratigraphy: *Constructional Moat* where reflections onlap at the slope side; *Mixed Moat* where reflections downlap at the bottom of the moat; and *Erosional Moat* where reflections are truncated at the drift side. It is suggested that some moats are driven by sediment erosion while others primarily exist due to differential sedimentation, meaning that less sediment is deposited inside the moat compared to the separated elongated mounded drift alongside the moat. From this study (at present day), 78% of the moats are Constructional Moats and are thus formed due to uneven sedimentation without erosive features.
- The Coriolis force has a significant control over the general ocean circulation. Its strength is dependent on the latitudes and current speed. However, our statistical analyses show no statistically significant correlation between latitude and the shape and size of moats. Thus, a multivariate analysis that includes more current speed measurements is necessary to determine better how the Coriolis force affects moat development.
- Our measurements from moats show a correlation between slope angle (adjacent to the emplacement of the moat) and drift angle. It is interpreted that the current is locally focused and intensified due to the steepness of the adjacent slope. This agrees with the measured current data. The authors hypothesize that a steeper slope focuses the current, resulting in a higher velocity gradient across the moat, which then leads to a steeper drift. Thus, the slope angle indirectly controls the drift angle and thereby the moat morphology. This clearly shows how the pre-existing morphology affects the ocean currents and associated sedimentation patterns.

ACKNOWLEDGEMENTS

We thank the captains, crews and onboard scientific teams for their work during cruise SO260 onboard *R/V SONNE* 2018, cruise PAMELA-MOZ2 onboard *R/V L'Atalante* in 2014, cruise PRISME2 onboard the *R/V L'Atalante* and cruise PRISME3 onboard the *R/V Pourquoi pas?* in 2013, cruise M95 onboard the *R/V Meteor* in 2013, cruise M84/4 onboard the *R/V Meteor* in 2011, *R/V Meteor* cruise M78/3 in 2009, cruise CADIPOR 1 + 2 onboard the *R/V Belgica* in 2002 and 2005 and cruise M49/2 onboard the *R/V Meteor* in 2001. The PAMELA-MOZ2 cruise was co-funded by TOTAL and IFREMER as part of the PAMELA project. The PAMELA (Passive Margin Exploration Laboratories) project is a scientific project led by IFREMER and TOTAL in collaboration with Université de Bretagne Occidentale, Université Rennes 1, Université Pierre and Marie Curie, CNRS and IFPEN. This study was carried out in collaboration with "The Drifters" Research Group at Royal Holloway University of London (RHUL). We thank TGS for their permission in using the seismic profile fragment for the Álvarez-Cabral Moat in Fig. 6C. We thank Ellen Unland (University Bremen) for processing the seismic data from the ET Moat 2 offshore Argentina. We thank the reviewers Uisdean Nicholson and Mathew Wells, Associate Editor Jeff Peakall and Chief Editor Piret Plink-Björklund for their constructive comments that greatly improved our manuscript. Open Access funding enabled and organized by Projekt DEAL.

DATA AVAILABILITY STATEMENT

The seismic data of this study from the ET Moat 2 offshore Argentina are available from the corresponding author upon reasonable request. The measured parameters from moat-drift systems for the statistical analyses are available on PANGAEA (Wilckens *et al.*, 2023; https://doi.org/10.1594/PANGAEA.955053). For all other data, sharing is not applicable to this article as it was previously published, and references are listed in Table S1 of the supplementary material.

REFERENCES

Allen, C., **Peakall, J.**, **Hodgson, D.**, **Bradbury, W.** and **Booth, A.** (2022) Latitudinal changes in submarine channel-levee system evolution, architecture and flow processes. *Front. Earth Sci.*, **10, 976852**.

Bailey, W.S., **McArthur, A.D.** and **McCaffrey, W.D.** (2021) Distribution of contourite drifts on convergent margins: examples from the Hikurangi subduction margin of New Zealand. *Sedimentology*, **68**, 294–323.

Betzler, C., **Lindhorst, S.**, **Eberli, G.P.**, **Lüdmann, T.**, **Möbius, J.**, **Ludwig, J.**, **Schutter, I.**, **Wunsch, M.**, **Reijmer, J.J.G.** and **Hübscher, C.** (2014a) Periplatform drift: the combined result of contour current and off-bank transport along carbonate platforms. *Geology*, **42**, 871–874.

Betzler, C., **Lindhorst, S.**, **Lüdmann, T.**, **von Borstel, F.**, **Büld, M.**, **Djamlan, E.**, **Eberli, G.**, **Eversheim, J.**, **Jentzen, A.**, **Keizer, F.**, **Ludwig, J.**, **Möbius, J.**, **Paulat, M.**, **Reiche, S.**, **Reijmer, J.**, **Reolid, J.**, **Schiebel, L.**, **Schutter, I.**, **Ulferts, L.**, **Winter, S.**, **Wolf, D.**, **Wunsch, M.**, **Rentsch, H.** and **Raeke, A.** (2014b) CICARB - cruise No. M95 - march 29 - April 25, 2013 - Kingston (Jamaica) - pointe à Pitre (Guadeloupe). In: *METEOR-Berichte (Meteor Cruise Reports)*, Vol. **M95**. DFG-Senatskommission für Ozeanographie, Bremen, 36 pp.

Cattaneo, A. (2013a) PRISME 2 cruise, RV L'Atalante. https://doi.org/10.17600/13010050.

Cattaneo, A. (2013b) PRISME 3 cruise, RV Pourquoi pas? https://doi.org/10.17600/13030060.

Cécile, R. and **Laurence, D.** (2014) PAMELA-MOZ02 cruise, RV L'Atalante. https://doi.org/10.17600/14001100.

Chen, H., **Zhang, W.**, **Xie, X.**, **Gao, Y.**, **Liu, S.**, **Ren, J.**, **Wang, D.** and **Su, M.** (2022) Linking oceanographic processes to contourite features: numerical modelling of currents influencing a contourite depositional system on the northern South China Sea margin. *Mar. Geol.*, **444**, 106714.

Clark, J.D., **Kenyon, N.H.** and **Pickering, K.T.** (1992) Quantitative analysis of the geometry of submarine channels: implications for the classification of submarine fans. *Geology*, **20**, 633–636.

Cossu, R., **Wells, M.G.** and **Wåhlin, A.K.** (2010) Influence of the Coriolis force on the velocity structure of gravity currents in straight submarine channel systems. *J. Geophys. Res. Oceans*, **115**, C11016.

Davarpanah Jazi, S., **Wells, M.G.**, **Peakall, J.**, **Dorrell, R.M.**, **Thomas, R.E.**, **Keevil, G.M.**, **Darby, S.E.**, **Sommeria, J.**, **Viboud, S.** and **Valran, T.** (2020) Influence of Coriolis force upon bottom boundary layers in a large-scale gravity current experiment: implications for evolution of sinuous deep-water channel systems. *J. Geophys. Res. Oceans*, **125**, e2019JC015284.

Deptuck, M.E. and **Sylvester, Z.** (2018) Submarine fans and their channels, levees, and lobes. In: *Submarine Geomorphology* (Eds Micallef, A., Krastel, S. and Savini, A.). Springer Geology. Springer, Cham.

Ercilla, G., **Juan, C.**, **Hernández-Molina, F.J.**, **Bruno, M.**, **Estrada, F.**, **Alonso, B.**, **Casas, D.**, **Farran, M.**, **Llave, E.**, **García, M.**, **Vázquez, J.T.**, **D'Acremont, E.**, **Gorini, C.**, **Palomino, D.**, **Valencia, J.**, **El Moumni, B.** and **Ammar, A.** (2016) Significance of bottom currents in deep-sea morphodynamics: an example from the Alboran Sea. *Mar. Geol.*, **378**, 157–170.

Faugères, J.C., **Stow, D.A.**, **Imbert, P.** and **Viana, A.** (1999) Seismic features diagnostic of contourite drifts. *Mar. Geol.*, **162**, 1–38.

García, M., **Hernández-Molina, F.J.**, **Llave, E.**, **Stow, D.A.V.**, **León, R.**, **Fernández-Puga, M.C.**, **Diaz del Río, V.** and **Somoza, L.** (2009) Contourite erosive features caused by the Mediterranean outflow water in the Gulf of Cadiz: quaternary tectonic and oceanographic implications. *Mar. Geol.*, **257**, 24–40.

Hanebuth, T.J.J. and **Cruise Participants**. (2011) Report and preliminary results of RV METEOR Cruise M84/4, GALIOMAR III, Vigo – Vigo. Berichte, Fachbereich Geowissenschaften, Universität Bremen, No. 283, 139 pages. Bremen, 2011.

Hanebuth, T.J., **Zhang, W.**, **Hofmann, A.L.**, **Löwemark, L.A.** and **Schwenk, T.** (2015) Oceanic density fronts steering bottom-current induced sedimentation deduced from a 50 ka contourite-drift record and numerical modeling (off NW Spain). *Quatern. Sci. Rev.*, **112**, 207–225.

Harris, P.T. and **Whiteway, T.** (2011) Global distribution of large submarine canyons: geomorphic differences between active and passive continental margins. *Mar. Geol.*, **285**, 69–86.

Hebbeln, D., **Van Rooij, D.** and **Wienberg, C.** (2016) Good neighbours shaped by vigorous currents: cold-water coral mounds and contourites in the North Atlantic. *Mar. Geol.*, **378**, 171–185.

Hernández-Molina, F.J., **Larter, R.D.**, **Rebesco, M.** and **Maldonado, A.** (2006) Miocene reversal of bottom water flow along the Pacific margin of the Antarctic peninsula: stratigraphic evidence from a contourite sedimentary tail. *Mar. Geol.*, **228**, 93–116.

Hernández-Molina, F.J., **Llave, E.** and **Stow, D.A.V.** (2008) Continental slope contourites. *Develop. Sedimentol.*, **60**, 379–408.

Hernández-Molina, F.J., **Stow, D.A.V.**, **Alvarez-Zarikian, C.A.**, **Acton, G.**, **Bahr, A.**, **Balestra, B.**, **Ducassou, E.**, **Flood, R.**, **Flores, J.A.**, **Furota, S.**, **Grunert, P.**, **Hodell, D.**, **Jimenez-Espejo, F.**, **Kim, J.K.**, **Krissek, L.**, **Kuroda, J.**, **Li, B.**, **Llave, E.**, **Lofi, J.**, **Lourens, L.**, **Miller, M.**, **Nanayama, F.**, **Nishida, N.**, **Richter, C.**, **Roque, C.**, **Pereira, H.**, **Sanchez Goni, M.F.**, **Sierro, F.J.**, **Singh, A.D.**, **Sloss, C.R.**, **Takashimizu, Y.**, **Tzanova, A.**, **Voelker, A.**, **Williams, T.** and **Xuan, C.** (2014) Onset of Mediterranean outflow in to the North Atlantic. *Science*, **344**, 1244–1250.

Hernández-Molina, F.J., **Sierro, F.J.**, **Llave, E.**, **Roque, E.**, **Stow, D.A.W.**, **William, T.**, **Lofi, J.**, **Vand der Schee, M.**, **Arnáiz, A.**, **Ledesma, S.**, **Rosales, C.**, **Rodriquez-Tovar, F.J.**, **Pardo-Igúzquiza, E.** and **Brackenridge, R.E.** (2016) Evolution of the gulf of Cadiz margin and Southwest

Portugal contourite depositional system: tectonic, sedimentary and paleoceanographic implications from IODP expedition 339. *Mar. Geol.*, **377**, 7–39.

Hiscott, R.N., **Hall, F.R.** and **Pirmez, C.** (1997) Turbidity-current overspill from the Amazon Channel: texture of the silt/sand load, paleoflow from anisotropy of magnetic susceptibility, and implications for flow processes. In: *Proceedings-Ocean Drilling Program Scientific Results* (Eds Flood, R.D., Piper, D.J.W., Klaus, A. and Peterson, L.C.), **155**, pp. 53–78. National Science Foundation.

Imran, J., **Parker, G.** and **Katopodes, N.** (1998) A numerical model of channel inception on submarine fans. *J. Geophys. Res. Oceans*, **103**, 1219–1238.

Kane, I.A., **Clare, M.A.**, **Miramontes, E.**, **Wogelius, R.**, **Rothwell, J.J.**, **Garreau, P.** and **Pohl, F.** (2020) Seafloor microplastic hotspots controlled by deep-sea circulation. *Science*, **368**, 1140–1145.

Kasten, S., **Schwenk, T.**, **Aromokeye, D.A.**, **Baques, M.**, **Baumann, K.-H.**, **Bergenthal, M.**, **Bösche, J.**, **Bozzano, G.**, **Brune, R.**, **Bülten, J.**, **Chiessi, C.M.**, **Coffinet, S.**, **Crivellari, S.**, **Garcia Chapori, N.**, **Gonzalez, L.**, **Hanebuth, T.J.J.**, **Hilgenfeldt, C.**, **Hüttich, D.**, **Jones, C.K.**, **Klann, M.**, **Klar, S.**, **Klein, T.**, **Kockisch, B.**, **Köster, M.**, **Lantzsch, H.**, **Linowski, E.**, **Long, J.H.**, **Melcher, A.-C.**, **Ogunleye, O.J.**, **Pereyra, N.**, **Rehage, R.**, **Riedinger, N.**, **Rosiak, U.**, **Schmidt, W.**, **Schnakenberg, A.**, **Spieß, V.**, **Steinmann, L.**, **Thieblemont, A.**, **Volz, J.**, **Warnke, F.**, **Warratz, G.**, **Wenau, S.** and **Zonneveld, K.A.F.** (2019) Dynamics of Sedimentation Processes and their Impact on Biogeochemical Reactions on the Continental Slope off Argentina and Uruguay (MARUM). Cruise No. SO260/Leg 1 & Leg 2, Leg 1: January 12–January 30, 2018, Buenos Aires (Argentina)-Montevideo (Uruguay), Leg 2: February 2-February, 14, 2018, Montevideo (Uruguay)-Buenos Aires (Argentina), DosProBio, Sonne-Berichte.

Lentz, S.J. and **Helfrich, K.R.** (2002) Buoyant gravity currents along a sloping bottom in a rotating fluid. *J. Fluid Mech.*, **464**, 251–278.

Liu, S., **Hernández-Molina, F.J.**, **Ercilla, G.** and **Van Rooij, D.** (2020) Sedimentary evolution of the Le Danois contourite drift systems (southern Bay of Biscay, NE Atlantic): a reconstruction of the Atlantic Mediterranean water circulation since the Pliocene. *Mar. Geol.*, **427**, 106217.

Llave, E., **Hernández-Molina, F.J.**, **Somoza, L.**, **Díaz-del-Río, V.**, **Stow, D.A.V.**, **Maestro, A.** and **Alveirinho Dias, J.M.** (2001) Seismic stacking pattern of the Faro-Albufeira contourite system (gulf of Cadiz): a quaternary record of paleoceanographic and tectonic influences. *Mar. Geophys. Res.*, **22**, 487–508.

Llave, E., **Hernández-Molina, F.J.**, **García, M.**, **Ercilla, G.**, **Roque, C.**, **Juan, C.**, **van Rooij, D.**, **Rebesco, M.**, **Brackenridge, R.**, **Jané, G.**, **Gómez-Ballesteros, M.** and **Stow, D.** (2020) Contourites along the Iberian continental margins: conceptual and economic implications. *Geol. Soc. Lond. Spec. Publ.*, **476**, 403–436.

Lüdmann, T., **Paulat, M.**, **Betzler, C.**, **Möbius, J.**, **Lindhorst, S.**, **Wunsch, M.** and **Eberli, G.P.** (2016) Carbonate mounds in the Santaren Channel, Bahamas: a current-dominated periplatform depositional regime. *Mar. Geol.*, **376**, 69–85.

McCave, I.N. and **Tucholke, B.E.** (1986) Deep current-controlled sedimentation in the western North Atlantic. In: *The Geology of North America, Vol. M, the Western North Atlantic Region* (Eds Vogt, P.R. and Tucholke, B.E.), Geological Society of America, Boulder, pp. 1117–1126.

McCave, I.N., **Manighetti, B.** and **Robinson, S.G.** (1995) Sortable silt and fine sediment size/composition slicing: parameters for palaeocurrent speed and palaeoceanography. *Paleoceanography*, **10**, 593–610.

McCave, I.N., **Thornalley, D.J.R.** and **Hall, I.R.** (2017) Relation of sortable silt grain-size to deep-sea current speeds: calibration of the 'mud current meter'. *Deep-Sea Res. I Oceanogr. Res. Pap.*, **127**, 1–12.

Miramontes, E., **Cattaneo, A.**, **Jouet, G.**, **Thereau, E.**, **Thomas, Y.**, **Rovere, M.**, **Cauquil, E.** and **Trincardi, F.** (2016) The Pianosa contourite depositional system (northern Tyrrhenian Sea): drift morphology and Plio-quaternary stratigraphic evolution. *Mar. Geol.*, **378**, 20–42.

Miramontes, E., **Garziglia, S.**, **Sultan, N.**, **Jouet, G.** and **Cattaneo, A.** (2018) Morphological control of slope instability in contourites: a geotechnical approach. *Landslides*, **15**, 1085–1095.

Miramontes, E., **Garreau, P.**, **Caillaud, M.**, **Jouet, G.**, **Pellen, R.**, **Hernández-Molina, F.J.**, **Clare, M.A.** and **Cattaneo, A.** (2019) Contourite distribution and bottom currents in the NW Mediterranean Sea: coupling seafloor geomorphology and hydrodynamic modelling. *Geomorphology*, **333**, 43–60.

Miramontes, E., **Jouet, G.**, **Thereau, E.**, **Bruno, M.**, **Penven, P.**, **Guerin, C.**, **Le Roy, P.**, **Droz, L.**, **Jorry, S.J.**, **Hernández-Molina, F.J.**, **Thiéblemont, A.**, **Jacinto, R.S.** and **Cattaneo, A.** (2020) The impact of internal waves on upper continental slopes: insights from the Mozambican margin (Southwest Indian Ocean). *Earth Surf. Process. Landf.*, **45**, 1469–1482.

Miramontes, E., **Thiéblemont, A.**, **Babonneau, N.**, **Penven, P.**, **Raisson, F.**, **Droz, L.**, **Jorry, S.J.**, **Fierens, R.**, **Counts, J.W.**, **Wilckens, H.**, **Cattaneo, A.** and **Jouet, G.** (2021) Contourite and mixed turbidite-contourite systems in the Mozambique Channel (SW Indian Ocean): link between geometry, sediment characteristics and modelled bottom currents. *Mar. Geol.*, **437**, 106502.

Mulder, T. (2011) Gravity processes and deposits on continental slope, rise and abyssal plains. *Deep-Sea Sed.*, **63**, 25–148.

Nicholson, U. and **Stow, D.** (2019) Erosion and deposition beneath the Subantarctic front since the early Oligocene. *Sci. Rep.*, **9**, 1–9.

Nicholson, U., **Libby, S.**, **Tappin, D.R.** and **McCarthy, D.** (2020) The Subantarctic front as a sedimentary conveyor belt for tsunamigenic submarine landslides. *Mar. Geol.*, **424**, 106161.

Paulat, M., **Lüdmann, T.**, **Betzler, C.** and **Eberli, G.P.** (2019) Neogene palaeoceanographic changes recorded in a carbonate contourite drift (Santaren Channel, Bahamas). *Sedimentology*, **66**, 1361–1385.

Peakall, J., **McCaffrey, B.** and **Kneller, B.** (2000) A process model for the evolution, morphology, and architecture of sinuous submarine channels. *J. Sediment. Res.*, **70**, 434–448.

Rebesco, M. (2005) Contourites R.C. In: *Encyclopedia of Geology* (Eds Selley, L.R.M. and Cocks, I.R.P.), pp. 513–527. Elsevier, Oxford.

Rebesco, M., **Hernández-Molina, F.J.**, **Van Rooij, D.** and **Wåhlin, A.** (2014) Contourites and associated sediments controlled by deep-water circulation processes: state-of-the-art and future considerations. *Mar. Geol.*, **352**, 111–154.

Rebesco, M., **Camerlenghi, A.**, **Munari, V.**, **Mosetti, R.**, **Ford, J.**, **Micallef, A.** and **Facchin, L.** (2021) Bottom current-

controlled quaternary sedimentation at the foot of the Malta escarpment (Ionian Basin, Mediterranean). *Mar. Geol.*, **441**, 106596.

Robin, C. and **Droz, L.** (2014) PAMELA-MOZ02 Cruise, RV L'Atalante. https://doi.org/10.17600/14001100.

Steinbrink, L., **Gohl, K.**, **Riefstahl, F.**, **Davy, B.** and **Carter, L.** (2020) Late cretaceous to recent ocean-bottom currents in the SW Pacific gateway, southeastern Chatham rise, New Zealand. *Palaeogeogr. Palaeoclimatol. Palaeoecol.*, **546**, 109633.

Stow, D.A. and **Mayall, M.** (2000) Deep-water sedimentary systems: new models for the 21st century. *Marine Petrol. Geol.*, **17**, 125–135.

Thiéblemont, A., **Hernández-Molina, F.J.**, **Miramontes, E.**, **Raisson, F.** and **Penven, P.** (2019) Contourite depositional systems along the Mozambique channel: the interplay between bottom currents and sedimentary processes. *Deep-Sea Res. I Oceanogr. Res. Pap.*, **147**, 79–99.

Tripsanas, E.K., **Panagiotopoulos, I.P.**, **Lykousis, V.**, **Morfis, I.**, **Karageorgis, A.P.**, **Anastasakis, G.** and **Kontogonis, G.** (2016) Late quaternary bottom-current activity in the South Aegean Sea reflecting climate-driven dense-water production. *Mar. Geol.*, **375**, 99–119.

Uenzelmann-Neben, G., **Weber, T.**, **Grützner, J.** and **Thomas, M.** (2017) Transition from the cretaceous ocean to Cenozoic circulation in the western South Atlantic—a twofold reconstruction. *Tectonophysics*, **716**, 225–240.

Van Keken, P.E., **Hacker, B.R.**, **Syracuse, E.M.** and **Abers, G.A.** (2011) Subduction factory: 4. Depth-dependent flux of H_2O from subducting slabs worldwide. *J. Geophys. Res. Solid Earth*, **116**, B01401.

Van Rensbergen, P., **Depreiter, D.**, **Pannemans, B.**, **Moerkerke, G.**, **Van Rooij, D.**, **Marsset, B.**, **Akhmanov, G.**, **Blinova, V.**, **Ivanov, M.**, **Rachidi, M.**, **Magalhães, V.**, **Pinheiro, L.M.**, **Cunha, M.** and **Henriet, J.P.** (2005) The El Arraiche mud volcano field at the Moroccan Atlantic slope, Gulf of Cadiz. *Marine Geol.*, **219**, 1–17.

Van Rooij, D., **Iglesias, J.**, **Hernández-Molina, F.J.**, **Ercilla, G.**, **Gomez-Ballesteros, M.**, **Casas, D.**, **Llave, E.**, **De Hauwere, A.**, **Garcia-Gil, S.**, **Acosta, J.** and **Henriet, J.P.** (2010) The Le Danois Contourite depositional system: interactions between the Mediterranean outflow water and the upper Cantabrian slope (north Iberian margin). *Mar. Geol.*, **274**, 1–20.

Vandorpe, T., **Van Rooij, D.** and **De Haas, H.** (2014) Stratigraphy and paleoceanography of a topography-controlled contourite drift in the pen Duick area, southern gulf of Cádiz. *Mar. Geol.*, **349**, 136–151.

Wells, M. and **Cossu, R.** (2013) The possible role of Coriolis forces in structuring large-scale sinuous patterns of submarine channel–levee systems. *Philos. Trans. R. Soc. A: Math. Phys. Eng. Sci.*, **371**, 20120366.

Wilckens, H., **Miramontes, E.**, **Schwenk, T.**, **Artana, C.**, **Zhang, W.**, **Piola, A.R.**, **Baques, M.**, **Provost, C.**, **Hernández-Molina, F.J.**, **Felgendreher, M.**, **Spieß, V.** and **Kasten, S.** (2021) The erosive power of the Malvinas current: influence of bottom currents on morpho-sedimentary features along the northern argentine margin (SW Atlantic Ocean). *Mar. Geol.*, **439**, 106539.

Wilckens, H., **Schwenk, T.**, **Lüdmann, T.**, **Betzler, C.**, **Zhang, W.**, **Chen, J.**, **Hernandéz-Molina, F.J.**, **Lefebvre, A.**, **Cattaneo, A.**, **Spieß, V.** and **Miramontes, E.** (2023) Morphological properties of moat-drift systems around the world. *PANGAEA*. https://doi.org/10.1594/PANGAEA.955053.

Wu, S., **Lembke-Jene, L.**, **Lamy, F.**, **Arz, H.W.**, **Nowaczyk, N.**, **Xiao, W.**, **Zhang, X.**, **Hass, H.C.**, **Titschack, J.** and **Kuhn, G.** (2021) Orbital-and millennial-scale Antarctic circumpolar current variability in Drake Passage over the past 140,000 years. *Nat. Commun.*, **12**, 1–9.

Wunsch, M., **Betzler, C.**, **Lindhorst, S.**, **Lüdmann, T.** and **Eberli, G.P.** (2017) Sedimentary dynamics along carbonate slopes (Bahamas archipelago). *Sedimentology*, **64**, 631–657.

Yin, S., **Hernández-Molina, F.J.**, **Zhang, W.**, **Li, J.**, **Wang, L.**, **Ding, W.** and **Ding, W.** (2019) The influence of oceanographic processes on contourite features: a multidisciplinary study of the northern South China Sea. *Mar. Geol.*, **415**, 105967.

Yin, S., **Hernández-Molina, F.J.**, **Lin, L.**, **Chen, J.**, **Ding, W.** and **Li, J.** (2021) Isolation of the South China Sea from the North Pacific subtropical gyre since the latest Miocene due to formation of the Luzon Strait. *Sci. Rep.*, **11**, 1–9.

Yu, K., **Miramontes, E.**, **Alves, T.M.**, **Li, W.**, **Liang, L.**, **Li, S.**, **Zhan, W.** and **Wu, S.** (2021) Incision of submarine channels over pockmark trains in the South China Sea. *Geophys. Res. Lett.*, **48**, e2021GL092861.

Zhang, W., **Hanebuth, T.J.** and **Stöber, U.** (2016) Short-term sediment dynamics on a meso-scale contourite drift (off NW Iberia): impacts of multi-scale oceanographic processes deduced from the analysis of mooring data and numerical modelling. *Mar. Geol.*, **378**, 81–100.

Zhao, Y., **Liu, Z.**, **Zhang, Y.**, **Li, J.**, **Wang, M.**, **Wang, W.** and **Xu, J.** (2015) In situ observation of contour currents in the northern South China Sea: applications for Deepwater sediment transport. *Earth Planet. Sci. Lett.*, **430**, 477–485.

Manuscript received 8 August 2022; revision accepted 21 February 2023

Supporting Information

Additional information may be found in the online version of this article:

Fig. S1. Diagrams showing correlations between (A) width and relief, (B) relief and latitude, (C) width and latitude, (D) relief-width ratio and latitude, (E) relief and moat water depth (F) width and moat water depth, (G) relief-width ratio and moat water depth, (H) relief and and slope angle, (I) width and slope angle and (J) relief-width ratio and and slope angle.

Table S1. Contourite moats reported in the literature from locations all over the world considered in this study (see Fig. 1) and key data used to quantify moat parameters.

